Supplementary data

Unexpected binding modes of inhibitors to the histone chaperone ASF1 revealed by a foldamer scanning approach

Marie E. Perrin,[†ab] Bo Li,[†c] Johanne Mbianda,[†c] May Bakail,[ab] Christophe André,[c] Gwenaëlle Moal,[ab] Pierre Legrand,[d] Virgine Ropars,[ab] Céline Douat,[c§] Françoise Ochsenbein*[ab] and Gilles Guichard*[c]

[a]Institute Joliot, Commissariat à l'énergie Atomique (CEA), Direction de la Recherche Fondamentale (DRF), CEA Saclay, 91191 Gif-sur-Yvette, France. E-mail: francoise.ochsenbein@cea.fr

[b]Institute for Integrative Biology of the Cell (I2BC), CEA, CNRS, Université Paris-Saclay, 91190 Gif-sur-Yvette, France

[c]Univ. Bordeaux, CNRS, Bordeaux INP, CBMN, UMR 5248, Institut Européen de Chimie et Biologie, 2 rue Robert Escarpit, 33607 Pessac, France. E-mail: g.guichard@iecb.u-bordeaux.fr

[d]Synchrotron SOLEIL, L'Orme des Merisiers, 91190 Gif-sur-Yvette, France

[§]Present address : Department of Pharmacy and Center for Integrated Protein Science, Ludwig-Maximillians-Universität, Butenandtstr. 5-13, 81377 München, Germany

†These authors contributed equally to this work

*Corresponding authors

This PDF file includes

	ASF1A$_N$–**P4** (8BV1)
Crystallization conditions	[ASF1A$_N$] = 7.1 mg/mL
	[ASF1A$_N$]:[**P4**] ratio = 1:1.5
	0.1 M Tris pH 8.5
	30% (w/v) PEG 400
Cryoprotection	12% (v/v) glycerol in mother liquor
Data collection	
Space group	*P4$_3$*
Cell dimensions	
a, *b*, *c* (Å)	123.89, 123.89, 179.31
α, β, γ (°)	90.0, 90.0, 90.0
Za	6x ASF1 protein
	6x inhibitor
Resolution (Å)	49.37-2.83 (2.91-2.83)*
R_{meas} ; R_{meas}#	0.16 (2.38)*; 0.18 (4.93)*
R_{pim} ; R_{pim}#	0.04 (0.64)* ; 0.05 (1.33)*
I/σI ; I/σI#	13.1 (1.4)* ; 19.3 (0.7)*
Completeness (%)	88.8 (22.5)*
Completeness (%)#	100 (100)*
Redundancy	14.3 (14.0)*
Redundancy#	14.3 (13.6)*
CC(1/2) ; CC(1/2)#	1.00 (0.61)* ; 1.00 (0.32)*
Refinement	
Resolution (Å)	29.79 (2.834)*
No. unique reflections	56834
R_{work} / R_{free} (%)	20.37 / 22.09
No. atoms	
Protein	7901
Heterogen	234
Water	148
***B*-factors**	
Protein	99.89
Heterogen	89.69
Water	76.59
R.m.s. deviations	
Bond lengths (Å)	0.008
Bond angles (°)	0.910
Molprobity	
Ramachandran outliers	0.00 %
Ramachandran favored	99.36 %
C-beta deviations	0

*Values in parentheses are for highest-resolution shell

Statistics after applying Staraniso

Supplementary Table S1 Data collection and statistical refinement of the crystal structures of ASF1A$_N$ in complex with the inhibitory peptide P4.

Compound	K_D (µM)	*N*	ΔH (kcal.mol^{-1})	-TΔS (kcal.mol^{-1})
P4	0.20 ± 0.09	1.0 ± 0.1	−9.2 ± 0.4	0.7 ± 0.6
c3u_3	7.7 ± 2.0	1.3 ± 0.1	-3.9 ± 0.5	-2.9 ± 0.7
c3u_4	18 ± 5	2.1 ± 0.3	-0.9 ± 0.2	-5.5 ± 0.4
c3u_5	4.0 ± 0.2	1.7 ± 0.1	-4.3 ± 0.3	-3.0 ± 0.3
c3u_6	8.0 ± 0.3	1.0 ± 0.1	-4.0 ± 0.2	-2.8 ± 0.1
c3u_7	12 ± 2	1.3 ± 0.2	-3.5 ± 0.1	-3.1 ± 0.1
c3u_8	45 ± 5	2.2 ± 0.3	-2.7 ± 0.2	-3.1 ± 0.3
c4u	2.7 ± 0.6	1.0 ± 0.1	−2.2 ± 0.1	−4.8 ± 0.2

Supplementary Table S2. Binding affinities and thermodynamic parameters of peptides/chimeras for ASF1A$_N$ as determined by ITC measurements. All along the manuscript, c3u_i stands for chimera containing 3 ureas whereas c4u is a chimera containing four ureas reported in a previous study. Results for c4u were previsously published. [1]

C3u_i chemical shift lists

C3u_3					C3u_5					C3u_7				
RESIDUE	atom	283°K	293°K	303°K	**RESIDUE**	atom	283°K	293°K	303°K	**RESIDUE**	atom	283°K	293°K	303°K
AC0	CA	24.51	24.56	24.59	**AC0**	CA	24.41	24.49	24.54	**AC0**	CA	24.518	24.635	24.573
	QA	2.07	2.07	2.07		QA	2.06	2.06	2.057		QA	2.1	2.099	2.087
E1	CA	57.28	57.30	57.33	**E1**	CA	57.08	57.109	57.246	**E1**	CA	57.70	57.73	57.66
	CB	30.21	30.19	30.23		CB	30.12	30.175	30.21		CB	30.03	30.14	30.11
	CG	36.25	36.27	36.32		CG	36.19	36.189	36.278		CG	36.17	36.24	36.24
	HA	4.14	4.14	4.15		HA	4.12	4.118	4.125		HA	4.13	4.14	4.14
	HN	8.51	8.45	8.38		HN	8.51	8.442	8.366		HG22	2.27	2.27	2.27
	N	127.24	127.19	127.04		N	127.7	127.47	127.35		HG23	2.23	2.23	2.23
	QB	1.94	1.95	1.95		QB	1.89	1.891	1.895		HN	8.55	8.476	8.419
	QG	2.23	2.23	2.23		QG	2.21	2.211	2.216		N	127.79	127.57	127.45
K2	CA	57.53	57.50	57.48	**K2**	CA	57.11	57.10	57.12	**K2**	CA	57.71	57.68	57.60
	CB	32.99	32.97	32.98		CB	32.58	32.57	32.59		CB	32.46	32.56	32.48
	CD	29.05	29.05	29.05		CD	29.00	29.01	29.01		CD	29.14	29.18	29.09
	CE	42.04	42.04	42.09		CE	42.05	42.03	42.03		CE	42.00	42.01	42.01
	CG	24.91	24.88	24.86		CG	24.68	24.63	24.64		CG	24.78	24.78	24.68
	HA	4.00	4.00	4.00		HA	4.06	4.06	4.05		HA	4.05	4.05	4.05
	HB2	1.46	1.44	1.42		HB2	1.48	1.47	1.47		HB2	1.59	1.57	1.55
	HB3	1.39	1.38	1.37		HB3	1.40	1.40	1.39		HB3	1.50	1.48	1.47
	HG2	1.18	1.16	1.15		HG2	1.13	1.12	1.11		HG2	1.19	1.17	1.15
	HG3	1.01	1.00	1.00		HG3	1.01	1.00	1.01		HG3	1.069	1.052	1.04
	HN	8.33	8.25	8.17		HN	8.45	8.37	8.30		HN	8.48	8.41	8.34
	N	121.92	121.74	121.56		N	121.33	121.13	120.96		N	121.08	120.93	120.78
	QD	1.53	1.52	1.52		QD	1.51	1.50	1.50		QD	1.55	1.53	1.52
	QE	2.86	2.86	2.86		QE	2.85	2.84	2.84		QE	2.85	2.85	2.85
NaL^{U}3	CA1	53.25	53.27	53.33	**NaL3**	CA	56.98	56.89	56.89	**NaL3**	CA	58.08	58.04	57.75
	CA2	46.68	46.69	46.73		CB	36.62	36.62	36.53		CB	36.35	36.35	36.31
	CB	37.56	37.50	37.47		HA	4.79	4.78	4.78		HA	4.66	4.68	4.68
	HA	4.38	4.37	4.38		HB2	3.71	3.71	3.71		HB2	3.67	3.67	3.688
	HA22	3.57	3.57	3.56		HB3	3.43	3.42	3.44		HB3	3.52	3.53	3.51
	HA23	3.13	3.13	3.15		HN	8.12	8.05	7.99		HN	8.21	8.13	8.06
	HB2	3.42	3.42	3.42		N	119.58	119.42	119.30		N	119.79	119.59	119.41
	HB3	3.06	3.07	3.08										
	HN1	7.86	7.79	7.72										
	HN2	6.18	6.15	6.11										
	N1	124.62	124.52	124.44										
	N2	79.31	79.41	79.48										
	CD1	130.38				CD1	130.56				CD1	130.58		
	CD3	129.24				CD3	129.44				CD3	129.44		
	CE1	128.35				CE1	128.40				CE1	128.46		
	CE3	128.73				CE3	128.92				CE3	128.91		
	CG2	126.09				CG2	125.87				CG2	125.77		
	CZ1	130.08				CZ1	130.66				CZ1	130.69		
	CZ2	131.62				CZ2	131.72				CZ2	131.71		
	HD1	7.38				HD1	7.40				HD1	7.42		
	HD3	7.59				HD3	7.62				HD3	7.62		
	HE1	7.45				HE1	7.46				HE1	7.48		
	HE3	7.56				HE3	7.58				HE3	7.57		
	HG2	8.11				HG2	8.11				HG2	8.09		
	HZ1	7.84				HZ1	7.87				HZ1	7.87		
	HZ2	7.95				HZ2	7.97				HZ2	7.96		
R^{U}4	CA1	52.76	52.78	52.82	**A4**	CA	53.28	53.25	53.24	**A4**	CA	53.72	53.74	53.68
	CA2	47.34	47.32	47.33		CB	19.59	19.70	19.75		CB	18.84	18.97	18.90
	CB	31.77	31.80	31.85		HA	4.20	4.20	4.20		HA	4.14	4.16	4.15
	CD	43.59	43.59	43.59		HN	8.19	8.12	8.04		HN	8.20	8.14	8.09
	CG	27.49	27.49	27.49		N	125.27	125.16	125.07		N	123.57	123.57	123.57
	HA	3.74	3.73	3.73		QB	1.40	1.39	1.38		QB	1.433	1.43	1.42
	HA22	3.30	3.30	3.29										
	HA23	2.77	2.81	2.82										
	HB2	1.49	1.50	1.50										
	HB3	1.33	1.33	1.33										
	HG2	1.65	1.65	1.65										
	HG3	1.55	1.55	1.55										
	HN1	6.00	5.96	5.92										

	HN2	5.98	5.94	5.92									
	HNE	7.25											
	N1	92.96	93.03	93.05									
	N2	79.89	79.92	79.92									
	NE	84.68											
	QD	3.15	3.14	3.14									
L^U5	CA1	50.96	51.03	51.13	**R^U5**	CA1	52.13	52.17	52.21	**R5**	CA	57.18	57.16	57.08
	CA2	47.55	47.46	47.55		CA2	46.65	46.56	46.59		CB	30.44	30.55	30.55
	CB	43.62	43.66	43.72		CB	31.20	31.24	31.27		CD	43.26	43.43	43.37
	CD1	23.97	23.92	23.99		CD	43.56	43.56	43.56		CG	27.40	27.45	27.39
	CD2	25.35	25.32	25.31		CG	27.58	27.56	27.56		HA	4.19	4.21	4.20
	CG	26.88	26.88	26.88		HA	3.94	3.92	3.91		HG2	1.68	1.68	1.67
	HA	3.65	3.65	3.64		HA22	3.30	3.29	3.28		HG3	1.61	1.60	1.60
	HA22	3.10	3.11	3.11		HA23	2.92	2.93	2.96		HN	8.12	8.074	8.02
	HA23	2.35	2.44	2.51		HB2	1.54	1.54	1.54		HNE	7.383	7.34	7.34
	HG	1.50	1.50	1.50		HB3	1.41	1.41	1.41		N	118.49	118.35	118.23
	HN1	5.77	5.76	5.73		HG2	1.63	1.62	1.62		NE	84.31	84.52	84.52
	HN2	6.09	6.08	6.07		HG3	1.54	1.54	1.54		QB	1.84	1.85	1.85
	N1	94.12	94.16	94.16		HN1	7.82	7.74	7.67		QD	3.20	3.20	3.20
	N2	82.02	82.09	82.07		HN2	5.93	5.91	5.89					
	QB	1.04	1.05	1.06		HNE	7.31	7.26	7.26					
	QD1	0.77	0.77	0.77		N1	125.08	124.99	124.89					
	QD2	0.79	0.79	0.79		N2	78.57	78.68	78.81					
						NE	85.10	84.98	84.98					
						QD	3.16	3.16	3.16					
A6	CA	53.22	53.24	53.26	**L^U6**	CA1	51.00	51.15	51.25	**L6**	CA	56.17	56.18	56.10
	CB	19.95	19.95	19.97		CA2	47.78	47.78	47.77		CB	42.62	42.70	42.71
	HA	4.06	4.07	4.07		CB	43.53	43.63	43.64		CD1	23.21	23.35	23.30
	HN	6.48	6.44	6.41		CD1	24.05	24.11	24.15		CD2	25.07	25.12	25.01
	N	91.24	91.32	91.37		CD2	25.23	25.26	25.27		HA	4.21	4.23	4.22
	QB	1.29	1.29	1.29		CG	27.03	27.03	27.03		HB2	1.65	1.64	1.63
						HA	3.80	3.77	3.76		HB3	1.51	1.51	1.52
						HA22	3.25	3.22	3.21		HN	8.01	7.95	7.89
						HA23	2.75	2.79	2.81		N	121.60	121.55	121.52
						HG	1.59	1.59	1.59		QD1	0.84	0.84	0.83
						HN1	5.90	5.85	5.81		QD2	0.85	0.85	0.85
						HN2	6.03	6.01	5.97		CG	26.95	26.95	26.95
						N1	93.96	94.06	94.13		HG	1.61	1.62	1.62
						N2	80.34	80.52	80.57					
						QB	1.21	1.21	1.21					
						QD1	0.84	0.83	0.83					
						QD2	0.85	0.85	0.85					
R7	CA	56.04	56.03	56.03	**Q^U7**	CA1	52.75	52.81	52.84	**Q^U7**	CA1	51.62	51.85	51.84
	CB	30.57	30.63	30.66		CA2	46.94	46.93	46.98		CA2	46.24	46.33	46.28
	CD	43.45	43.45	43.39		CB	30.97	30.95	30.91		CB	29.83	29.93	29.92
	CG	27.31	27.31	27.31		CG	34.41	34.41	34.50		CG	34.06	34.22	34.16
	HA	4.29	4.30	4.30		HA	3.66	3.65	3.66		HA	3.85	3.87	3.87
	HB2	1.87	1.87	1.86		HA22	3.32	3.30	3.30		HA22	3.25	3.26	3.25
	HB3	1.76	1.76	1.75		HA23	2.91	2.92	2.94		HA23	2.72	2.79	2.80
	HG2	1.63	1.64	1.64		HB2	1.72	1.731	1.73		HB2	1.65	1.69	1.69
	HG3	1.58	1.56	1.56		HB3	1.47	1.49	1.50		HB3	1.33	1.41	1.42
	HN	8.44	8.37	8.31		HN1	5.91	5.88	5.85		HN1	7.64	7.60	7.56
	HNE	7.25				HN2	6.42	6.38	6.35		HN2	5.94	5.94	5.91
	N	118.47	118.38	118.21		HNE2	7.46	7.42	7.38		HNE2	7.38	7.34	7.30
	NE	84.52				HNE3	6.75	6.72	6.69		HNE3	6.79	6.74	6.70
	QD	3.17	3.16	3.18		N1	91.79	91.81	91.84		N1	124.30	124.40	124.47
						N2	82.02	82.00	81.99		N2	79.18	79.18	79.24
						NE	112.42	112.14	111.85		NE	112.31	112.02	111.72
						QG	2.18	2.18	2.21		QG	2.11	2.15	2.15
R8	CA	56.33	56.36	56.36	**R8**	CA	57.14	57.14	57.24	**R^U8**	CA1	52.96	53.04	52.97
	CB	30.79	30.77	30.74		CB	31.46	31.48	31.48		CA2	47.27	47.25	47.18
	CD	43.42	43.42	43.42		CD	43.35	43.34	43.38		CB	31.72	31.84	31.79
	CG	27.13	27.13	27.13		CG	27.32	27.32	27.32		CD	43.46	43.69	43.65
	HA	4.27	4.28	4.28		HA	4.12	4.11	4.12		CG	27.66	27.66	27.62
	HB2	1.82	1.83	1.84		HB2	1.75	1.75	1.75		HA	3.70	3.70	3.69
	HB3	1.75	1.76	1.75		HB3	1.67	1.67	1.67		HA22	3.34	3.33	3.31

	HG2	1.61	1.61	1.61		HN	6.62	6.57	6.52		HA23	2.79	2.83	2.84
	HG3	1.57	1.57	1.57		HNE	7.26	7.25	7.25		HB2	1.51	1.51	1.50
	HN	8.43	8.39	8.32		N	88.19	88.23	88.29		HB3	1.31	1.33	1.32
	HNE	7.24				NE	84.34	84.58	84.58		HG2	1.61	1.61	1.61
	N	122.78	122.59	122.48		QD	3.13	3.13	3.14		HG3	1.52	1.54	1.53
	NE	84.65				QG	1.55	1.54	1.54		HN1	5.94	5.90	5.86
	QD	3.16	3.16	3.16							HN2	5.97	5.96	5.95
											HNE	7.18	7.15	7.15
											N	93.04	93.06	93.03
											N2	79.72	79.72	79.64
											NE	85.07	85.21	85.21
											QD	3.12	3.13	3.13
	CA	60.95	60.98	61.01		CA	61.01	61.03	61.05		CA1	56.83	57.05	57.04
	CB	38.82	38.86	38.90		CB	38.74	38.77	38.80		CA2	44.82	44.89	44.81
	CD	12.81	12.81	12.86		CD	12.87	12.85	12.89		CD	13.41	13.41	13.44
	CG1	27.21	27.20	27.21		CG1	27.30	27.32	27.32		CG1	27.48	27.48	27.47
	CG2	17.39	17.45	17.50		CG2	17.49	17.48	17.52		CG2	17.78	17.85	17.78
	HA	4.16	4.16	4.16		HA	4.16	4.162	4.16		HA	3.60	3.59	3.58
	HB	1.87	1.87	1.87		HB	1.89	1.89	1.89		HA22	3.47	3.45	3.43
	HG12	1.48	1.47	1.47		HG12	1.47	1.46	1.46		HA23	2.80	2.85	2.85
I9	HG13	1.18	1.18	1.18	**I9**	HG13	1.18	1.18	1.18	**$I^{U}9$**	HB12	1.43	1.43	1.42
	HN	8.32	8.22	8.13		HN	8.23	8.16	8.09		HG13	1.09	1.09	1.08
	N	123.33	122.91	122.54		N	120.93	120.62	120.36		HN1	5.97	5.94	5.91
	QD	0.86	0.86	0.86		QD	0.86	0.86	0.86		HN2	6.15	6.13	6.10
	QG2	0.92	0.92	0.91		QG2	0.92	0.91	0.91		N1	91.77	91.72	91.71
											N2	81.27	81.36	81.45
											QD	0.86	0.85	0.84
											QG2	0.88	0.88	0.87
	CA	52.38	52.35	52.33		CA	52.42	52.34	52.32		CA	52.61	52.70	52.66
	CB	19.42	19.48	19.55		CB	19.47	19.40	19.40		CB	20.17	20.27	20.22
	HA	4.25	4.27	4.28		HA	4.25	4.25	4.27		HA	4.11	4.12	4.12
A10	HN	8.48	8.39	8.30	**A10**	HN	8.49	8.42	8.32	**A10**	HN	6.59	6.54	6.49
	N	129.24	128.95	128.66		N	128.64	128.17	128.17		N	92.70	92.69	92.65
	QB	1.39	1.39	1.39		QB	1.38	1.37	1.37		QB	1.33	1.34	1.33
	HN2	7.62				HN2	7.57	7.50	7.44		HN2	7.90	7.82	7.75
AM11	HN3	7.11			**AM11**	HN3	7.12	7.06	7.00	**AM11**	HN3	7.12	7.05	6.99
	N	106.95				N	106.74	106.48	106.21		N	106.41	106.16	105.90

Supplementary Table S3. Chemical shift assignments of c3u_3, c3u_5 and c3u_7. Chemical sifhts are referenced with DSS. Spectra were recorded at 283°K, 293°K, 303°K in 10mM phosphate buffer pH 6. Atom names are indicated in Fig. S4E.

c3u_3.

Residue *i* *(O-atom)*	Number *i*	Residue *j*	H-atom	Number *j*	Intramolecular H-bond (*i*←*j*)	(Pseudo)cyclic conformation
NAC	0	**Nal^{U}**	HN2	3	1←4	C_{13}
Glu	1	**Nal^{U}**	HN2	3	1←3	C_{10}
Lys	2	**Arg^{U}**	HN2	4	1←3	C_{12}
Lys	2	**Leu^{U}**	HN1	5	1←4	C_{14}
Nal^{U}	3	**Leu^{U}**	HN2	5	1←3	C_{12}
Nal^{U}	3	**Ala**	HN	6	1←4	C_{14}
Arg^{U}	4	**Arg**	HN	7	1←4	C_{10}
Leu^{U}	5	**Arg**	HN	8	1←4	C_{10}
Leu^{U}	5	**Ile**	HN	9	1←5	C_{13}
Ala	6	**Ile**	HN	9	1←4	C_{10}
Ala	6	**ALN**	HN1	10	1←5	C_{13}
Arg	7	**ALN**	HN2	10	1←4	C_{13}
Arg	8	**ALN**	HN2	10	1←4	C_{10}

c3u_5.

Residue *i* *(O-atom)*	Number *i*	Residue *j*	H-atom	Number *j*	Intramolecular H-bond (*i*←*j*)	(Pseudo)cyclic conformation
NAC	0	**Nal**	HN	3	1←4	C_{10}
NAC	0	**Ala**	HN	4	1←5	C_{13}
Glu	1	**Arg^{U}**	HN1	5	1←5	C_{13}
Lys	2	**Arg^{U}**	HN1	5	1←4	C_{10}
Lys	2	**Arg^{U}**	HN2	5	1←4	C_{13}
Nal	3	**Arg^{U}**	HN2	5	1←3	C_{10}
Nal	3	**Leu^{U}**	HN1	6	1←4	C_{12}
Ala	4	**Leu^{U}**	HN2	6	1←3	C_{12}
Ala	4	**Gln^{U}**	HN1	7	1←4	C_{14}
Arg^{U}	5	**Gln^{U}**	HN2	7	1←3	C_{12}
Arg^{U}	5	**Arg**	HN	8	1←4	C_{14}
Leu^{U}	6	**Ile**	HN	9	1←4	C_{12}
Gln^{U}	7	**ALN**	HN1	10	1←4	C_{10}
Gln^{U}	7	**ALN**	HN2	10	1←4	C_{13}

c3u_7.

Residue *i* *(O-atom)*	Number *i*	Residue *j*	H-atom	Number *j*	Intramolecular H-bond (*i*←*j*)	(Pseudo)cyclic conformation
NAC	0	**Nal**	HN	3	1←4	C_{10}
NAC	0	**Ala**	HN	4	1←5	C_{13}
Glu	1	**Arg**	HN	5	1←5	C_{13}
Lys	2	**Arg**	HN	5	1←4	C_{10}
Lys	2	**Leu**	HN	6	1←5	C_{13}
Nal	3	**Leu**	HN	6	1←4	C_{10}
Nal	3	**Gln^{U}**	HN1	7	1←5	C_{13}
Ala	4	**Gln^{U}**	HN1	7	1←4	C_{10}
Ala	4	**Gln^{U}**	HN2	7	1←4	C_{13}
Arg	5	**Gln^{U}**	HN2	7	1←3	C_{10}
Arg	5	**Arg^{U}**	HN1	8	1←4	C_{12}
Leu	6	**Arg^{U}**	HN2	8	1←3	C_{12}
Leu	6	**Ile^{U}**	HN1	9	1←4	C_{14}
Gln^{U}	7	**Ile^{U}**	HN2	9	1←3	C_{12}
Gln^{U}	7	**ALN**	HN1	10	1←4	C_{14}

Supplementary Table S4. Intramolecular hydrogen-bond network within models of straigth helical c3u chimeras cu3_3, cu3_5 and cu3_7. In helices formed exclusively by α-amino acid building blocks, two major types of conformations are populated: the C_{10} conformation (a 3.0_{10}-helix stabilized by 1←4 intramolecular H-bonds) and the C_{13} conformation (a 3.6_{13}- or α-helix stabilized by 1←5 intramolecular H-bonds). Standard *N,N'*-linked oligourea segment displays an intramolecular H-bonding pattern characterized by the simultaneous presence of 12- and 14-membered pseudorings resulting from CO*i*···HN*i*+2 and CO*i*···HN*i*+3 connectivities, so 1←3 and 1←4 hydrogen bonds, respectively.

	ASF1A$_N$–**c3u_3** (8CJ1)	ASF1A$_N$–**c3u_5** (8CJ2)	ASF1A$_N$–**c3u_7** (8CJ3)
Crystallization conditions	[ASF1A$_N$] = 7.1 mg/mL [ASF1A$_N$]:[**u_3**] ratio = 1:3 0.1 M MES pH 6.5 40% (w/v) PEG 200	[ASF1A$_N$] = 7.1 mg/mL [ASF1A$_N$]:[**u_5**] ratio = 1:2 0.17 M ammonium sulfate 0.085 M NaOAc pH 4.6 25.5% PEG 2000 MME 15% (v/v) glycerol	[ASF1A$_N$] = 7.1 mg/mL [ASF1A$_N$]:[**u_7**] ratio = 1:3 0.2 M potassium fluoride 20% (w/v) PEG 3350
Data collection			
Space group	$P2_12_12_1$	$P6_2$	$P6_4$
Cell dimensions			
a, *b*, *c* (Å)	91.56, 93.23, 227.68	98.67, 98.67, 168.56	133.91, 133.91, 63.43
α, β, γ (°)	90.0, 90.0, 90.0	90.0, 90.0, 120.0	90.0, 90.0, 120.0
Za	8x ASF1 protein 4x inhibitor	4x ASF1 protein 4x inhibitor	1x ASF1 protein 1x inhibitor
Resolution (Å)	88.27-2.56 (2.63-2.56)*	49.34-2.13 (2.18-2.13)*	46.05-3.00 (3.08-3.00)*
R_{meas} ; R_{meas}#	0.41 (1.07)* ; 0.68 (4.36)*	0.11 (1.59)* ; 0.11 (1.59)*	0.18 (3.11)* ; 0.23 (9.32)*
R_{pim} ; R_{pim}#	0.11 (0.49)* ; 0.14 (0.94)*	0.02 (0.36)* ; 0.02 (0.36)*	0.04 (0.66)* ; 0.05 (2.03)*
I/σI ; I/σI#	6.8 (1.6)* ; 5.6 (0.7)*	20.1 (2.0)* ; 19.6 (2.0)*	17.1 (1.1)* ; 13.3 (0.3)*
Completeness (%)	57.8 (2.5)*	98.8 (96.8)*	80.1 (24.6)*
Completeness (%)#	98.8 (83.6)*	99.8 (96.8)*	99.9 (99.9)*
Redundancy	13.3 (14.1)*	21.2 (18.8)*	20.4 (21.9)*
Redundancy#	24.7 (19.9)*	21.2 (18.8)*	20.3 (20.6)*
CC(1/2) ; CC(1/2)#	0.99 (0.32)* ; 0.99 (0.32)*	1.00 (0.77)* ; 1.00 (0.75)*	1.00 (0.57)* ; 1.00 (0.40)*
Refinement			
Resolution (Å)	27.88 (2.52)*	24.41 (2.13)*	29.61 (3.00)*
No. unique reflections	36876	51870	10553
R_{work} / R_{free} (%)	22.51 / 27.99	19.33 / 21.50	20.27 / 21.69
No. atoms			
Protein	10060	5110	1282
Heterogen	34	318	58
Water	301	349	16
***B*-factors**			
Protein	47.94	56.25	74.46
Heterogen	78.53	73.54	80.65
Water	23.24	55.33	55.83
R.m.s. deviations			
Bond lengths (Å)	0.008	0.008	0.008
Bond angles (°)	0.900	0.920	0.920
Molprobity			
Ramachandran outliers	0.00 %	0.00 %	0.00 %
Ramachandran favored	98.28 %	99.34 %	99.35 %
C-beta deviations	0	3	0

*Values in parentheses are for highest-resolution shell

#Statistics after applying Staraniso

Supplementary Table S5. Data collection and statistical refinement of the crystal structures of ASF1A$_N$ in complex with the inhibitory chimeras c3_u3, c3u_5 and c3u_7.

Chimeras	Sequences	Yield	MS (ESI)	
			Calculated $[M+3H]^{3+}$	Found $[M+3H]^{3+}$
c3u_3	Ac-Glu-Lys-Nal^{U}-Arg^{U}-Leu^{U}-Ala-Arg-Arg-Ile-Ala-NH_2	28%	479.9686	479.9150
c3u_4	Ac-Glu-Lys-Nal-Ala^{U}-Arg^{U}-Leu^{U}-Arg-Arg-Ile-Ala-NH_2	57%	479.9686	479.9729
c3u_5	Ac-Glu-Lys-Nal-Ala-Arg^{U}-Leu^{U}-Gln^{U}-Arg-Ile-Ala-NH_2	19.6%	470.6211	470.6304
c3u_6	Ac-Glu-Lys-Nal-Ala-Arg-Leu^{U}-Gln^{U}-Arg^{U}-Ile-Ala-NH_2	22.7%	470.6211	470.6311
c3u_7	Ac-Glu-Lys-Nal-Ala-Arg-Leu-Gln^{U}-Arg^{U}-Ile^{U}-Ala-NH_2	20.3%	470.6211	470.6288
c3u_8	Ac-Glu-Lys-Nal-Ala-Arg-Leu-Ala-Gln^{U}-Arg^{U}-Ile^{U}-NH_2	43.3%	470.6211	470.6312

Supplementary Table S6. List of the 3-urea chimeras (c3u_i) synthesized and results of yield after purification and MS.

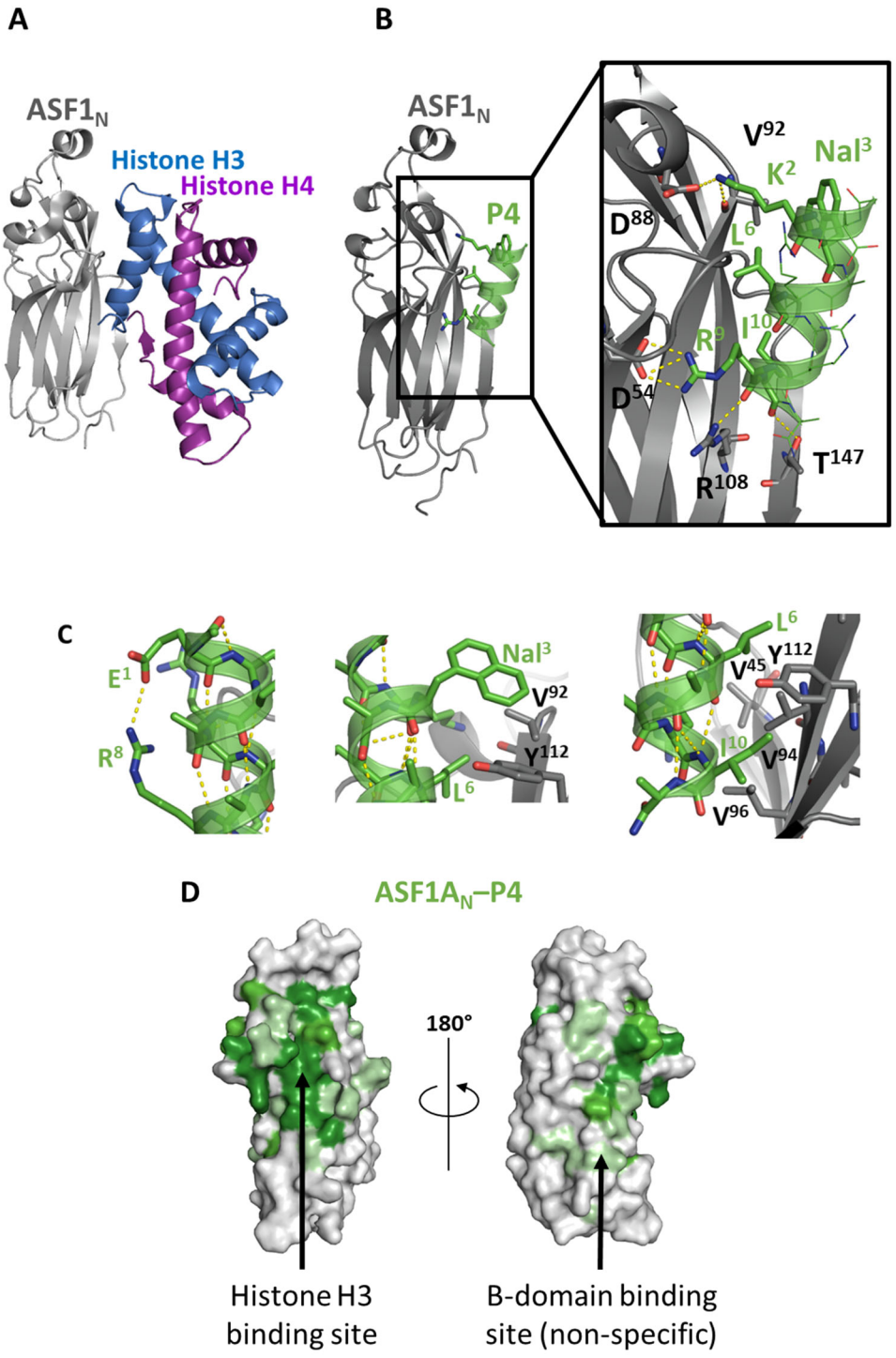

Supplementary Figure S1. X-ray structure of the complex ASF1A$_N$–P4. ***(A)*** Structure of the ternary complex hASF1A(1-154)–H3–H4 (PDB code: 2io5). ASF1A$_N$ is represented in dark grey, histone H3 and H4 in blue and purple respectively. **(*B) left panel***, global view of the ASF1A$_N$–**P4** interface characterized by a 1:1 interaction. ASF1A$_N$ is represented in dark grey, and **P4** residues in green. ***Right panel***, zoomed view. Hotspots residues of **P4** inhibitor (three letter code) as well as amino acids of ASF1A$_N$ (one letter code) are highlighted (representation in sticks and cartoon). ***(C)*** Details on intra- and intermolecular interactions. Hydrogen bonds are shown with yellow dashed lines. ***(D)*** Chemical shift mapping after the addition of an excess of **P4** inhibitor (ASF1:P4 ratio = 1:2). The chemical shift variations per residue are coloured in green according to the following code: dark (Δδ≥0.21 ppm), medium (0.14≤Δδ<0.21 ppm), light (0.07≤Δδ<0.14 ppm), grey (Δδ<0.07 ppm) (representation in surface).

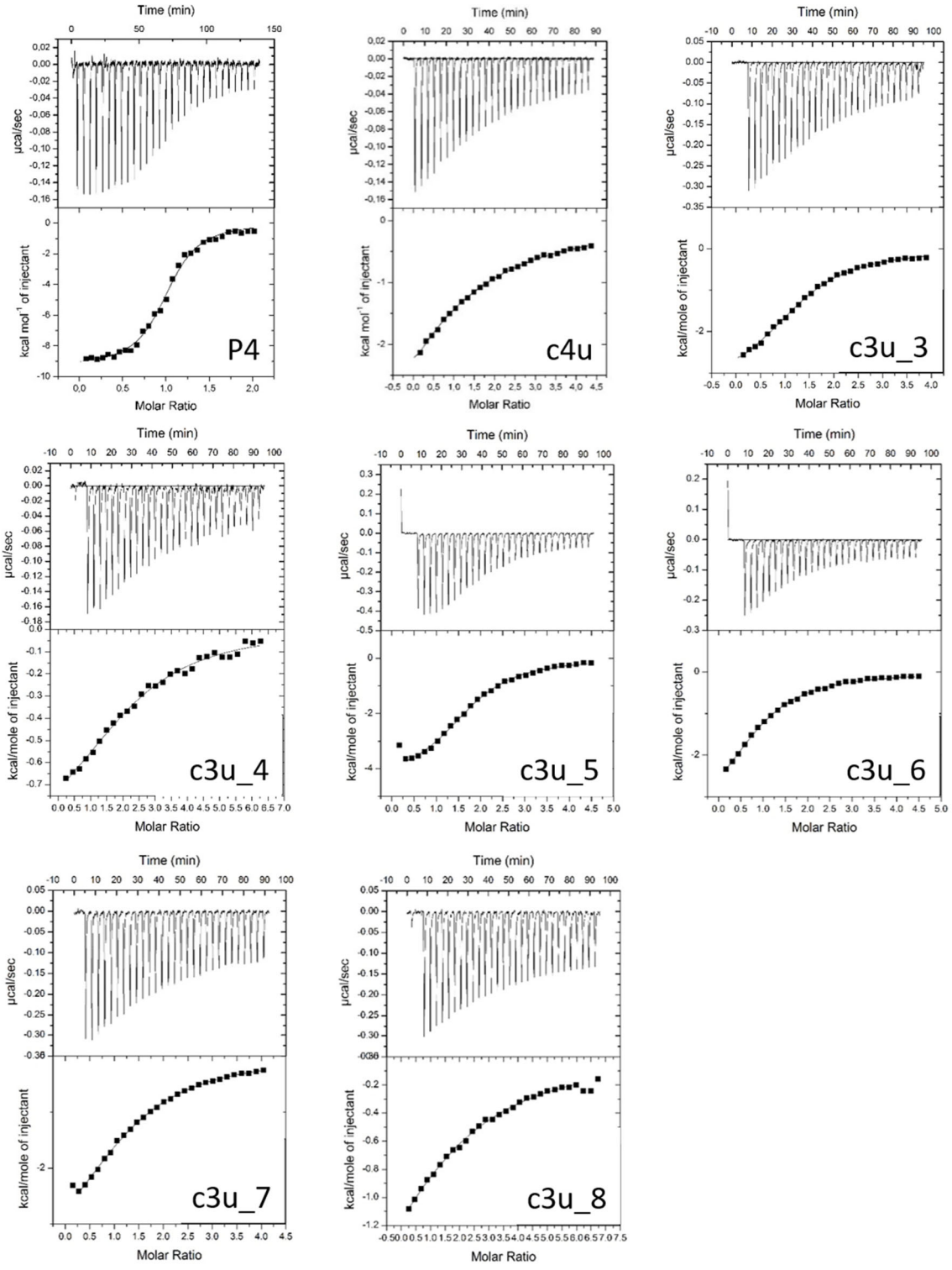

Supplementary Figure S2. ITC thermograms and data fitting for the indicated peptides/chimera upon titration of ASF1A$_N$.

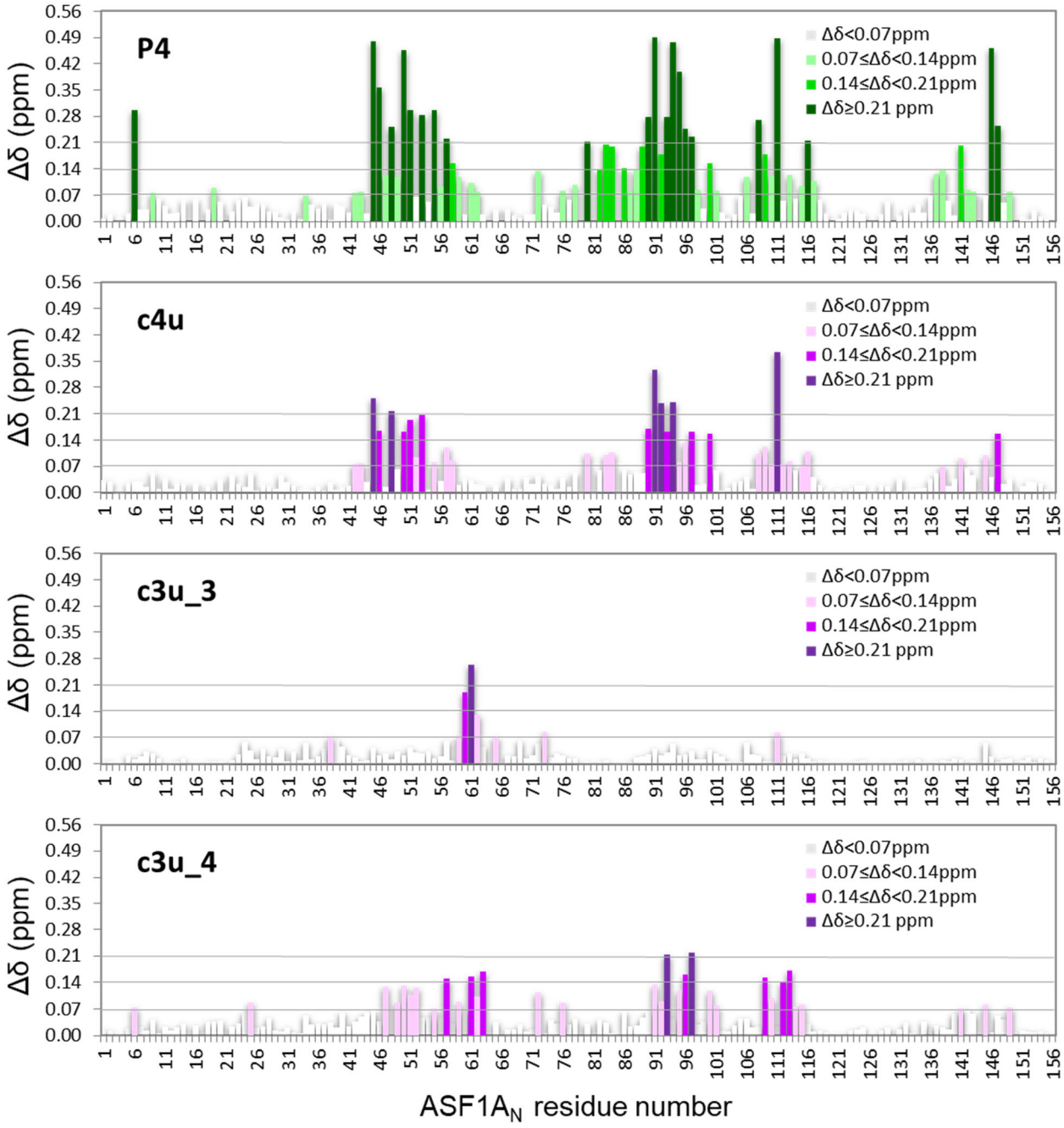
P4
c4u
c3u_3
c3u_4
Δδ (ppm)
Δδ<0.07ppm
0.07≤Δδ<0.14ppm
0.14≤Δδ<0.21ppm
Δδ≥0.21 ppm
ASF1A$_N$ residue number

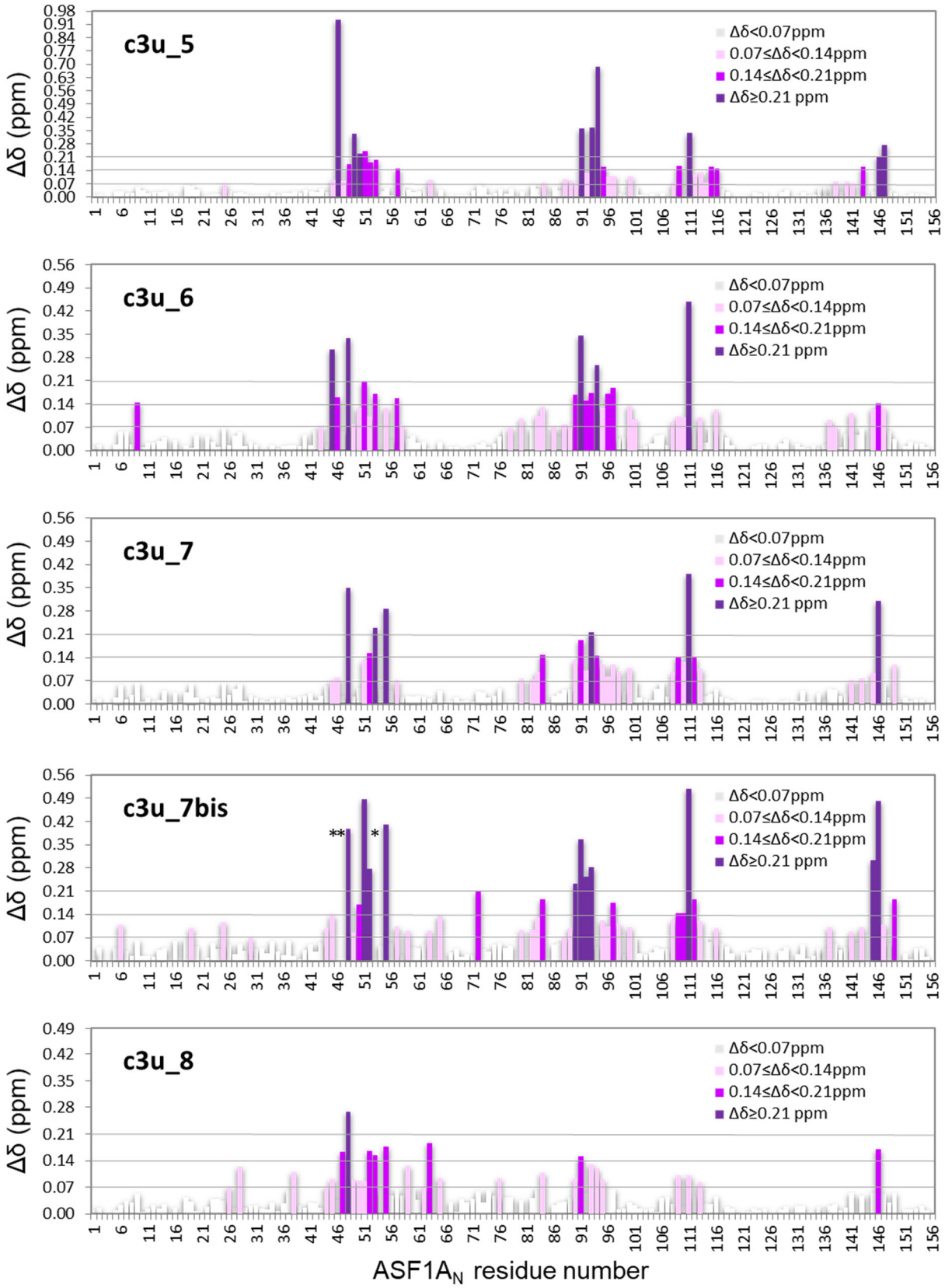

Supplementary Figure S3A. NMR titration of ASF1A$_N$: chemical shift perturbations (CSP) observed after the addition of an excess of the indicated peptide or chimera (ASF1A$_N$:inhibitor ratio = 1:2). Chemical shift changes of residues are highlighted with the following colour code (in green for peptides and in magenta or orange for chimeras, respectively): dark colour Δδ≥0.21 ppm, medium colour 0.14≤Δδ<0.21 ppm, light colour 0.07≤Δδ<0.14 ppm, grey Δδ<0.07 ppm.

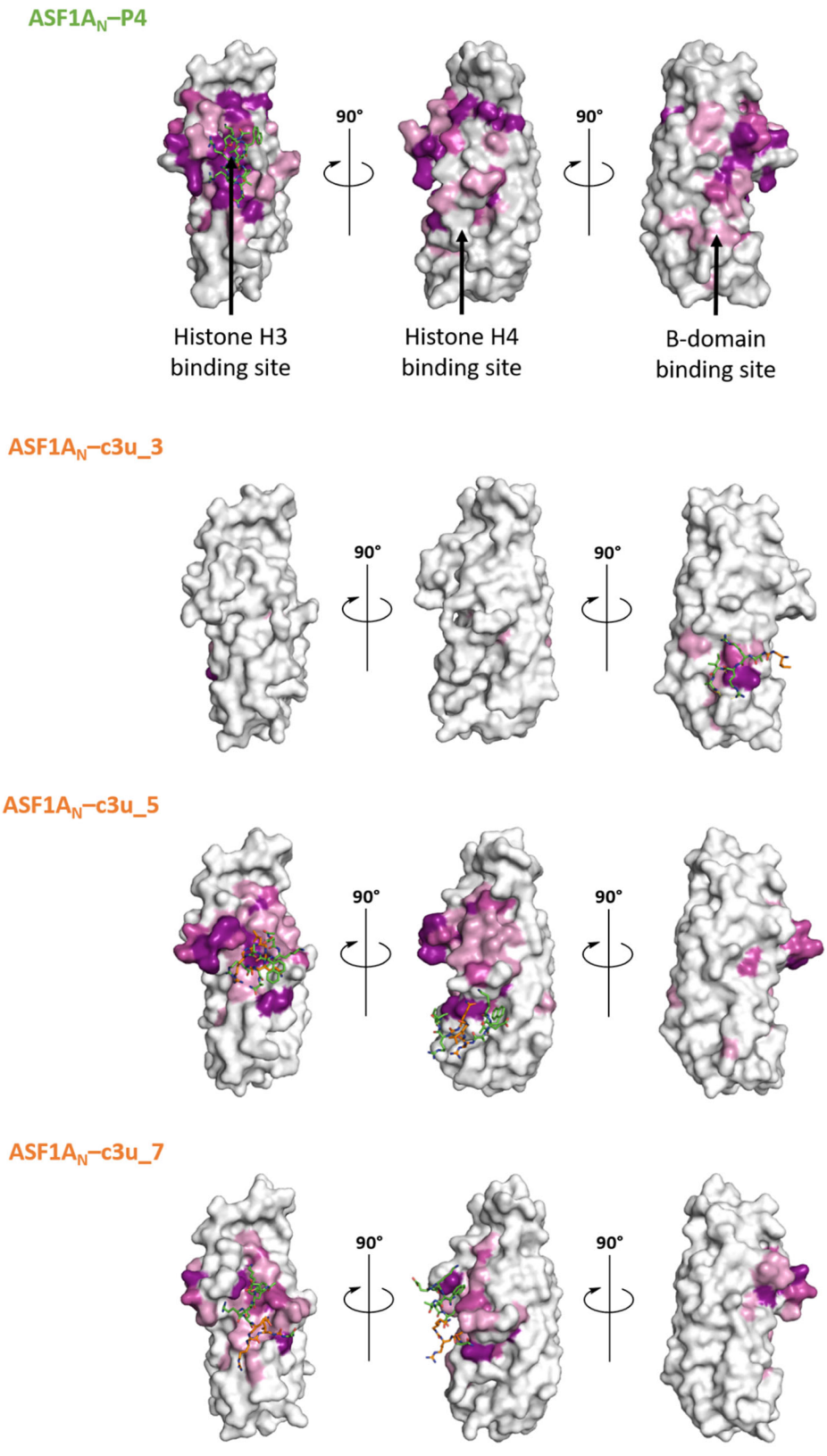

Supplementary Figure S3B. Chemical shift mapping after the addition of an excess of peptide or chimera inhibitor. ASF1A$_N$ is represented in light grey and inhibitor residues as in Figure 2. ASF1:inhibitor ratio = 1:2. The chemical shift variations per residue are coloured in purple according to the following code: dark ($\Delta\delta \geq 0.21$ ppm), medium ($0.14 \leq \Delta\delta < 0.21$ ppm), light ($0.07 \leq \Delta\delta < 0.14$ ppm), grey ($\Delta\delta < 0.07$ ppm) (representation in surface).

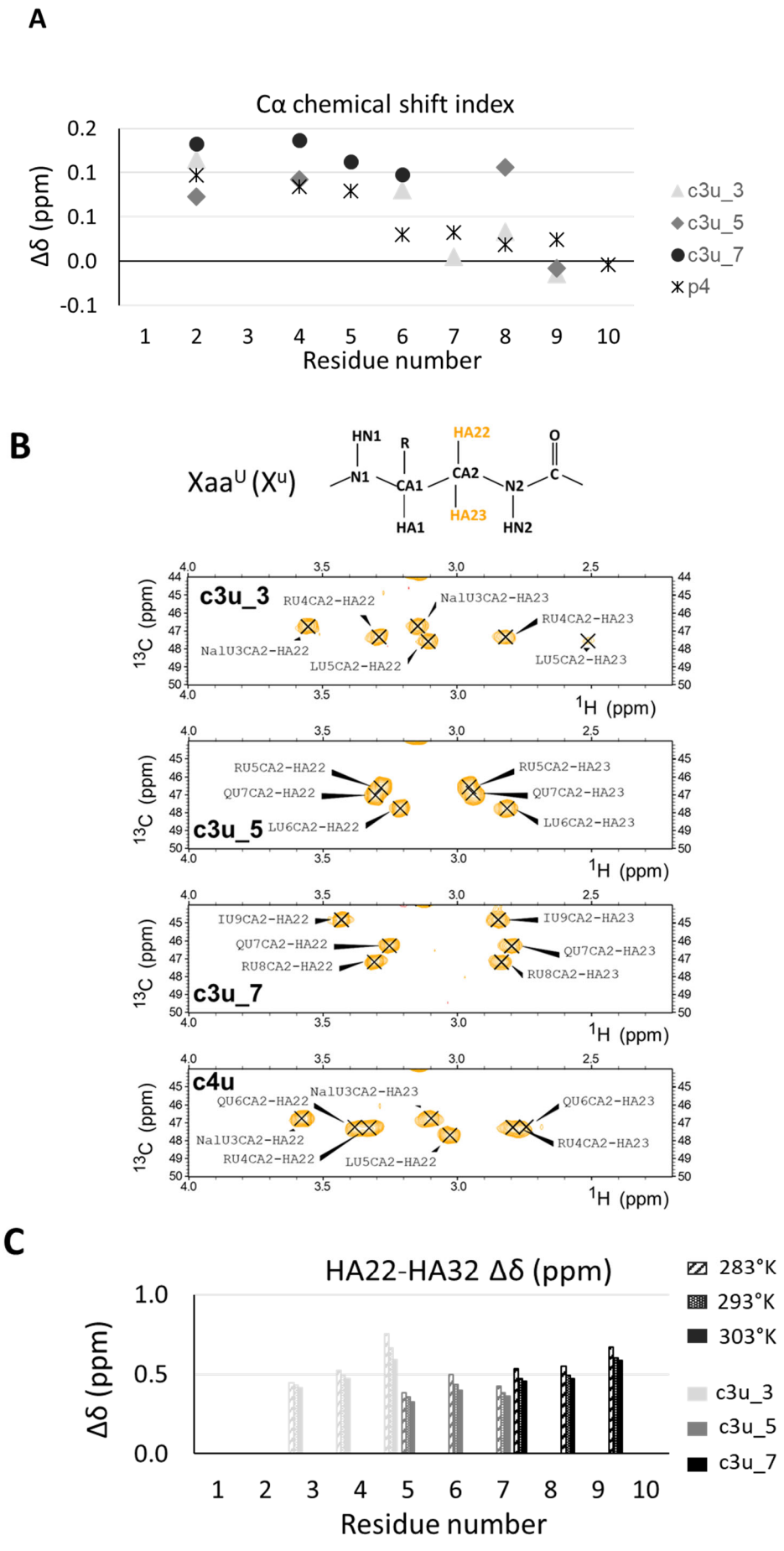

Supplementary Figure S4. NMR parameters showing the helical conformation of P4, c3u_3, c3_5 c3u_7 and c4u chimera *(A-C)*. ***(A)*** chemical shift indexes (CSI) along the chimera sequences for α-amino acid residues[2] as measured in 10mM phosphate buffer pH

6, at 283°K. ***(B)*** Zoom of the ^{13}C HSQC spectra of chimera in the region corresponding to the diastereoisotopic HA22 and HA23 of urea residues in 10mM phosphate buffer pH 6, at 303°K. ***(C)*** Measurement of the chemical shift difference between HA22 and HA23 protons of the three c3u chimera at three temperatures.

D

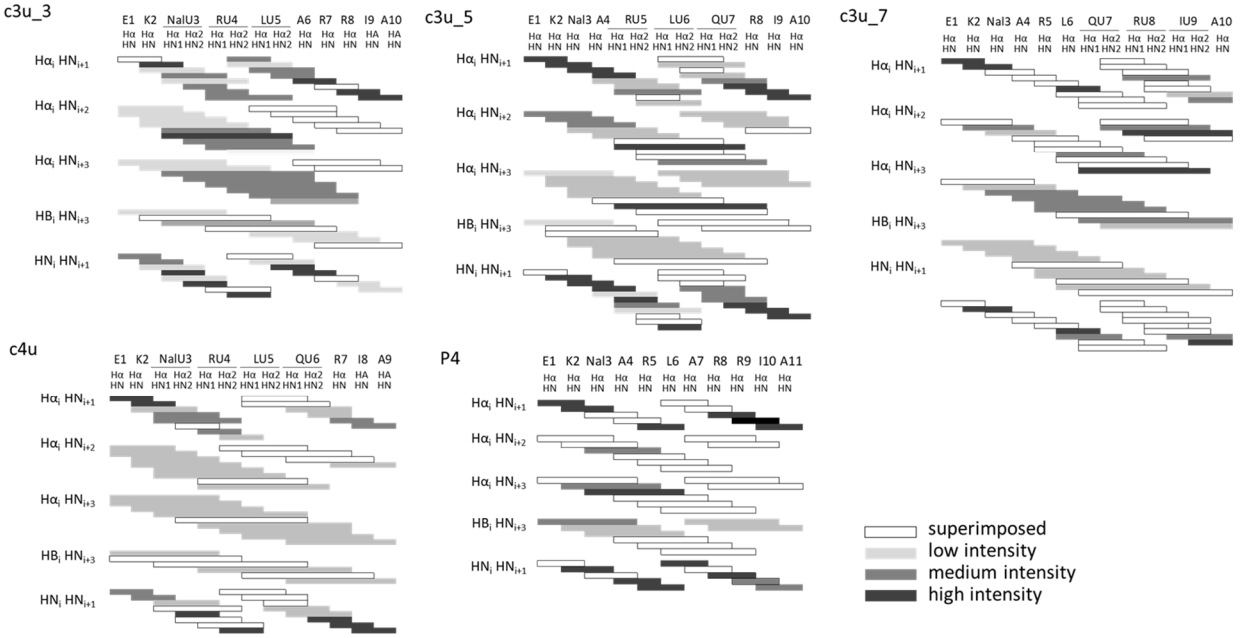

Supplementary Figure S4. NMR parameters supporting the helical conformation of P4, as well as c3u_3, c3_5 c3u_7 and c4u chimera *(D)*. Sequencial NOE correlations observed for the free chimeras in 10mM phosphate buffer pH 6, at 283°K and comparison with those of **C4u** and peptide **P4**.

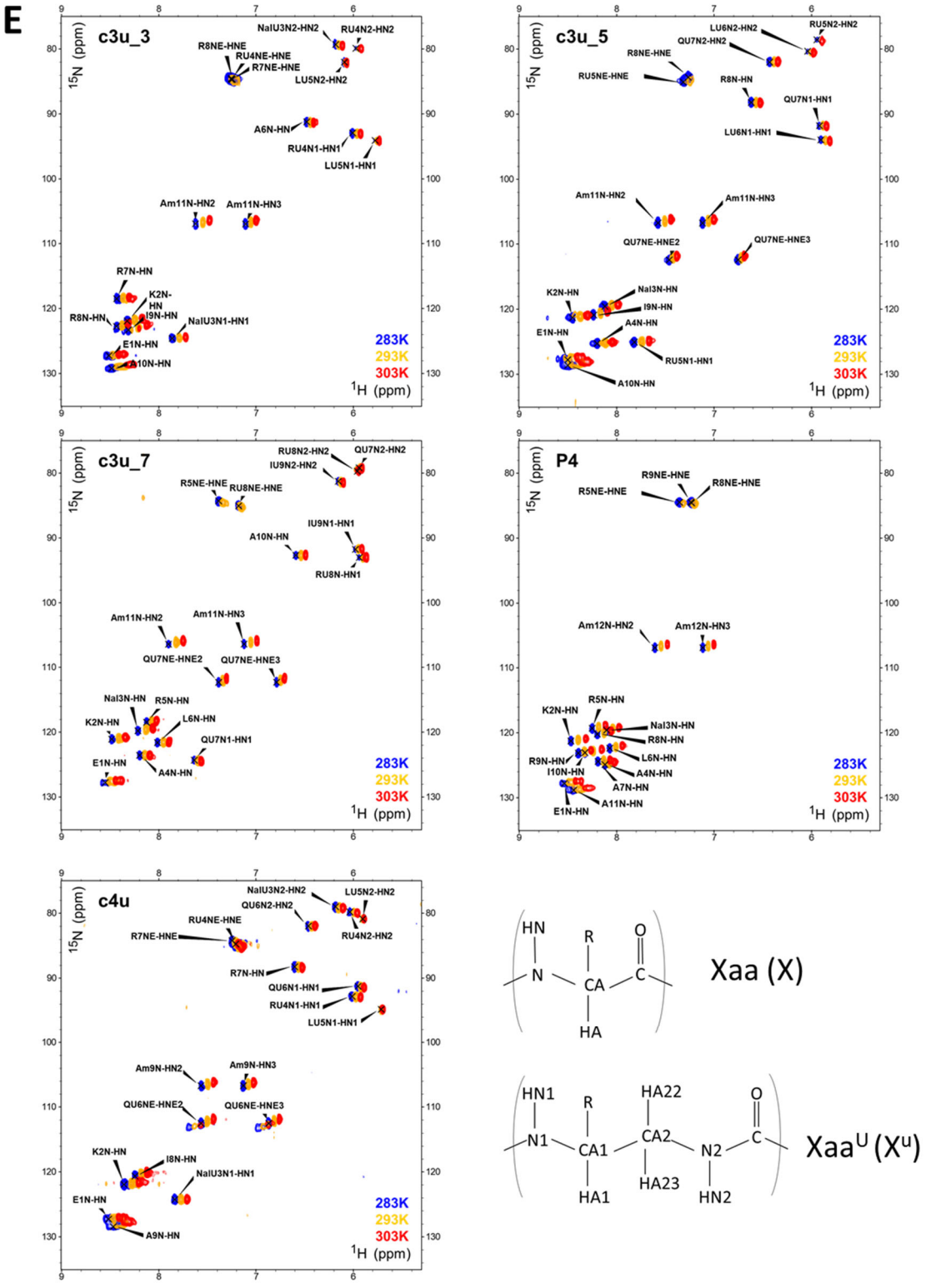

Supplementary Figure S4. NMR parameters showing the helical conformation of peptide P4 and c3u_3, c3_5 c3u_7 and c4u chimeras *(E)*. Sofast HMQC spectra of chimera recorded at three different temperatures. The assignment was done according to the atom names indicated in the lower right panel. Atom names of the side chains are identical to those of the corresponding amino-acid.

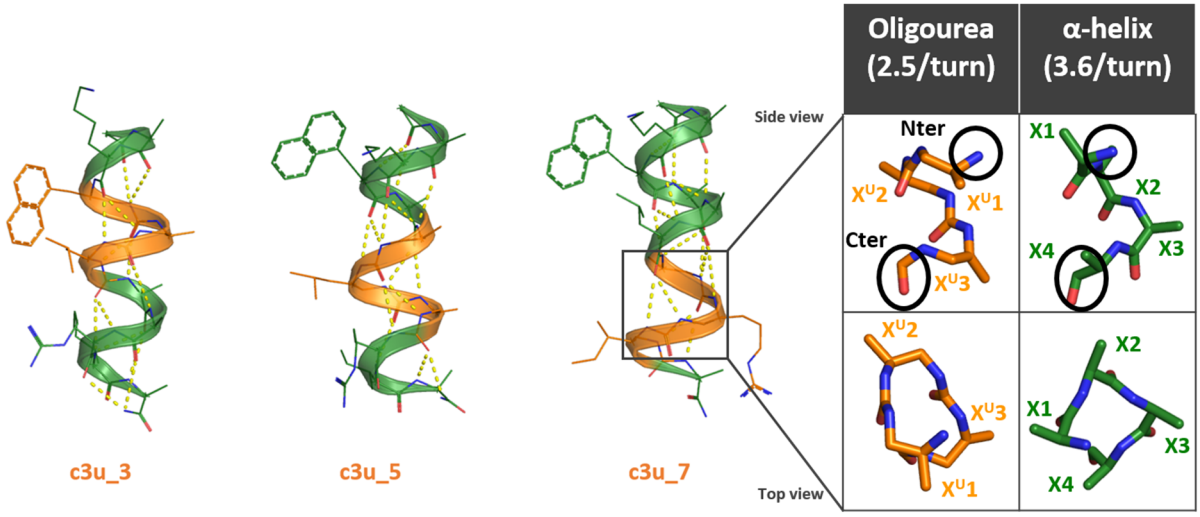

Supplementary Figure S5. Structure representation of *in silico* models for c3u_3, c3_5 and c3u_7 chimera inhibitors. ***Side views***, the oligourea segment is assumed to favour the transition from a "random coil" to α-helix, *i.e.* it increases the "propensity" of the primary sequence to adopt a helical conformation. ***Top-views***, a focus on the projections of side-chains in both helices. The number of residues per helix turn is indicated at the top of the table.

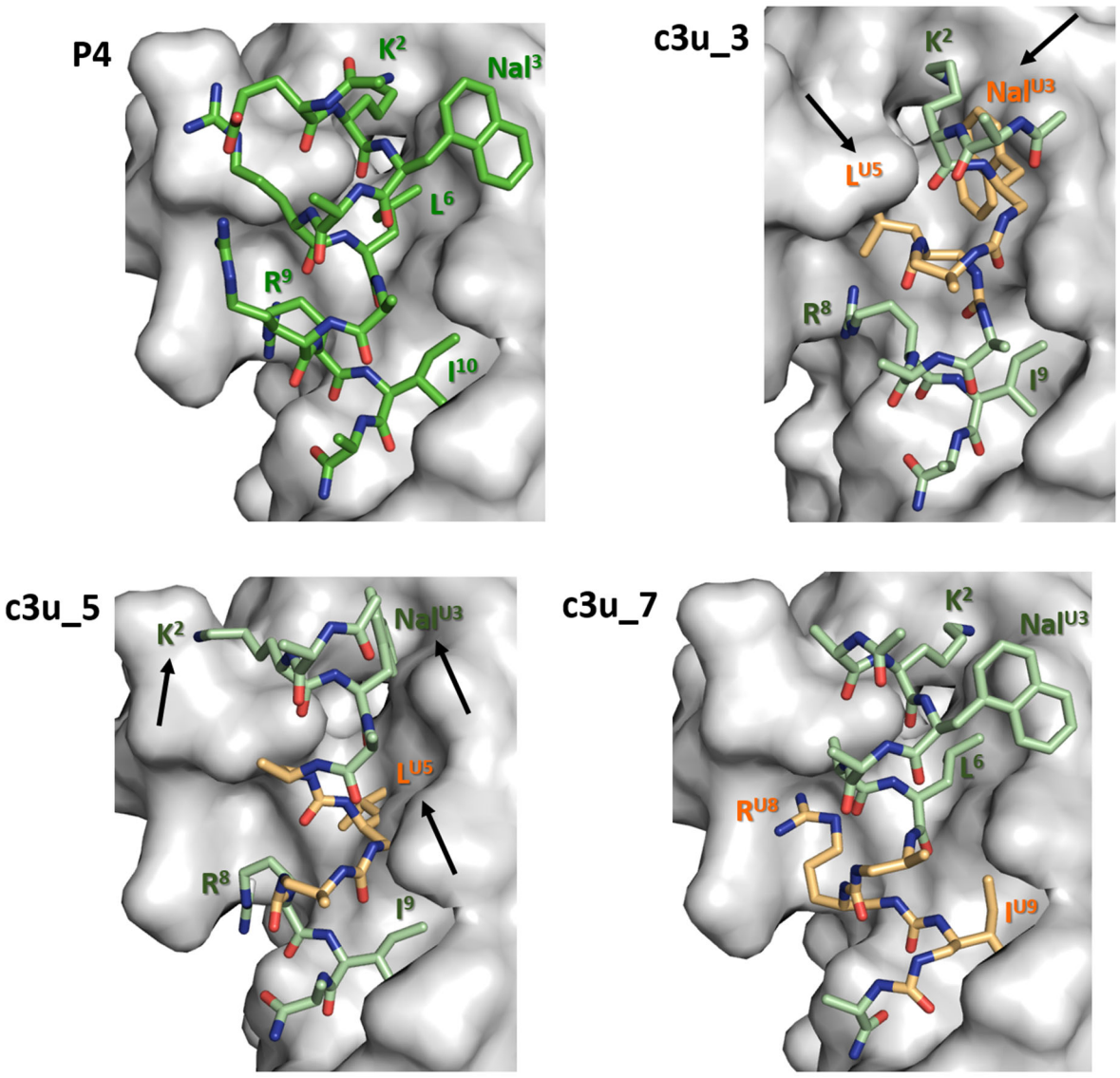

Supplementary Figure S6. *In silico* modelling of c3u_3, c3u_5 and c3_7 bound at the surface of the ASF1A$_N$–P4 complex. ASF1 is coloured in grey. The chimera inhibitors are coloured according to Figure 2. A pair fitting of the *in silico* straight helix model of **c3u_3**, **c3u_5** and **c3_7** (see Fig. S4) was performed on the **P4** helix. Residues that clash at the surface of ASF1 are indicated with black arrows (representation in sticks and cartoon).

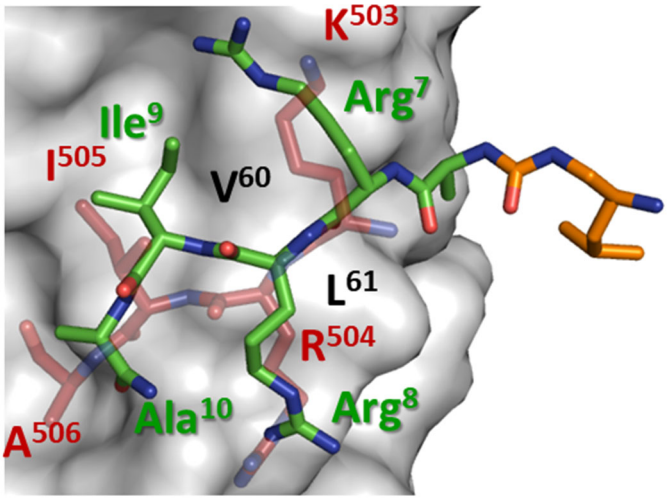

Supplementary Figure S7. The chimera c3u_3 is structured as a β-strand upon binding to ASF1 that superimposes well with B domains. Superimposition of X-ray crystal structure of **c3u_3** bound to ASF1 with the structure of the peptide chain of Cac2 (light red) bound to ASF1 (PDB code: 2Z3F). ASF1 is represented in grey surface. Residues are labelled in black, the chimera inhibitor is coloured according to Figure 2 and Figure 3.

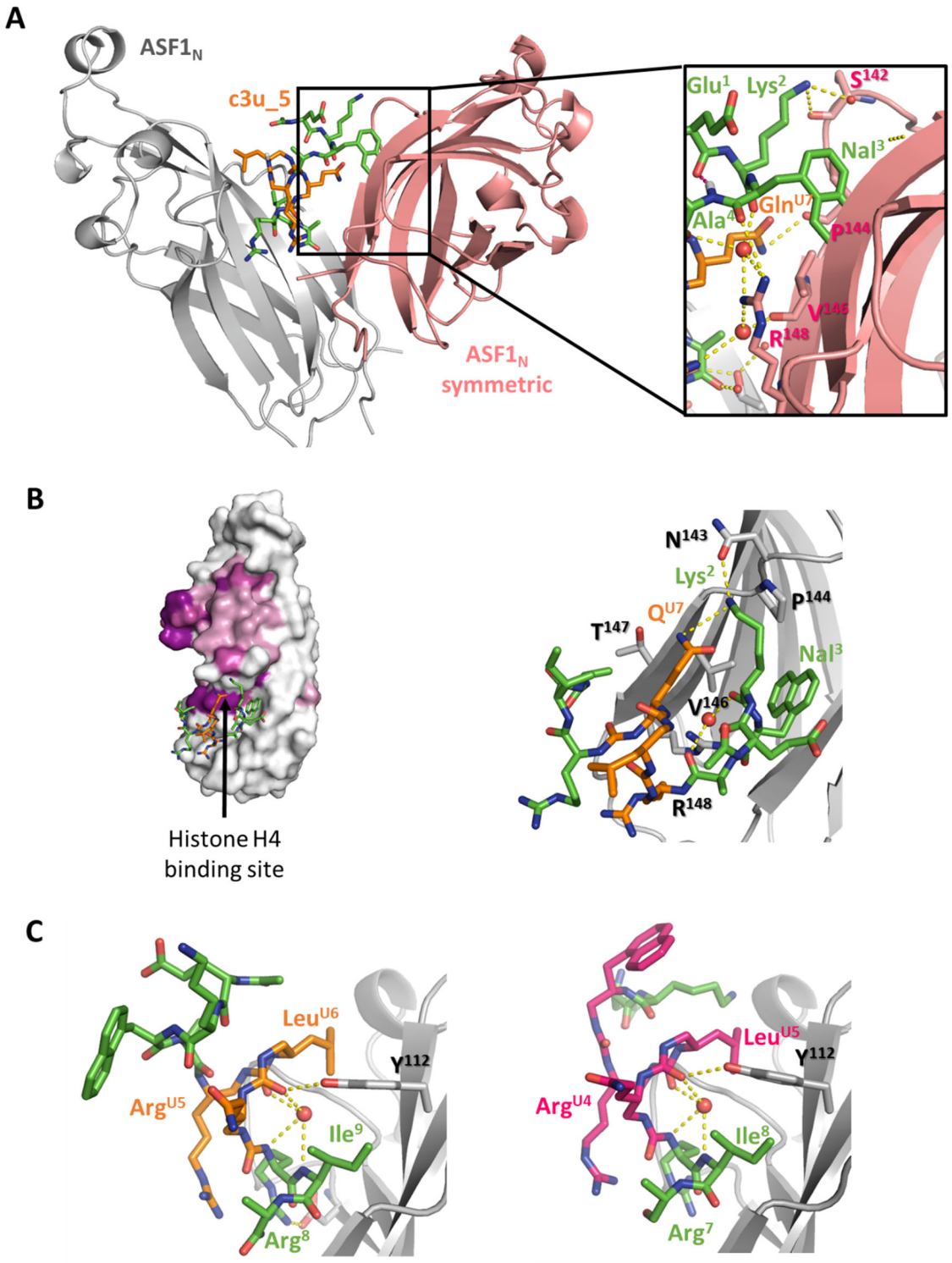

Supplementary Figure S8. X-ray structure of the complex ASF1A$_N$–c3u_5 (full complex). ASF1 is represented in grey (main chain) and in salmon (symmetric), the chimera inhibitor is coloured according to Figure 2. Hydrogen bonds are shown with yellow dashed lines. ***(A) Left panel***, the chimera **c3u_5** interacts with two chains of ASF1 in the crystal lattice. ***Right panel***, zoomed view. Details on intra- and intermolecular interactions. The α-amino acid residues of the symmetric chain are highlighted in dark pink. Hydrogen bonds are shown with yellow dashed lines. Selected water molecules are shown with red spheres. ***(B)*** Views in the regions of the H4 binding pocket. ***(C)*** Binding mode similarities between ASF1A$_N$-**c3u_**5 and ASF1A$_N$-**c4u** complex x-ray crystal structures. The water molecule bridging both inhibitors to the surface of ASF1 is depicted as a red sphere (representation in sticks and cartoon). ***Left panel***, ASF1A$_N$-**c3u_5** complex. ***Right panel***, ASF1A$_N$-**c4u** complex (PDB code: 6ZUF).

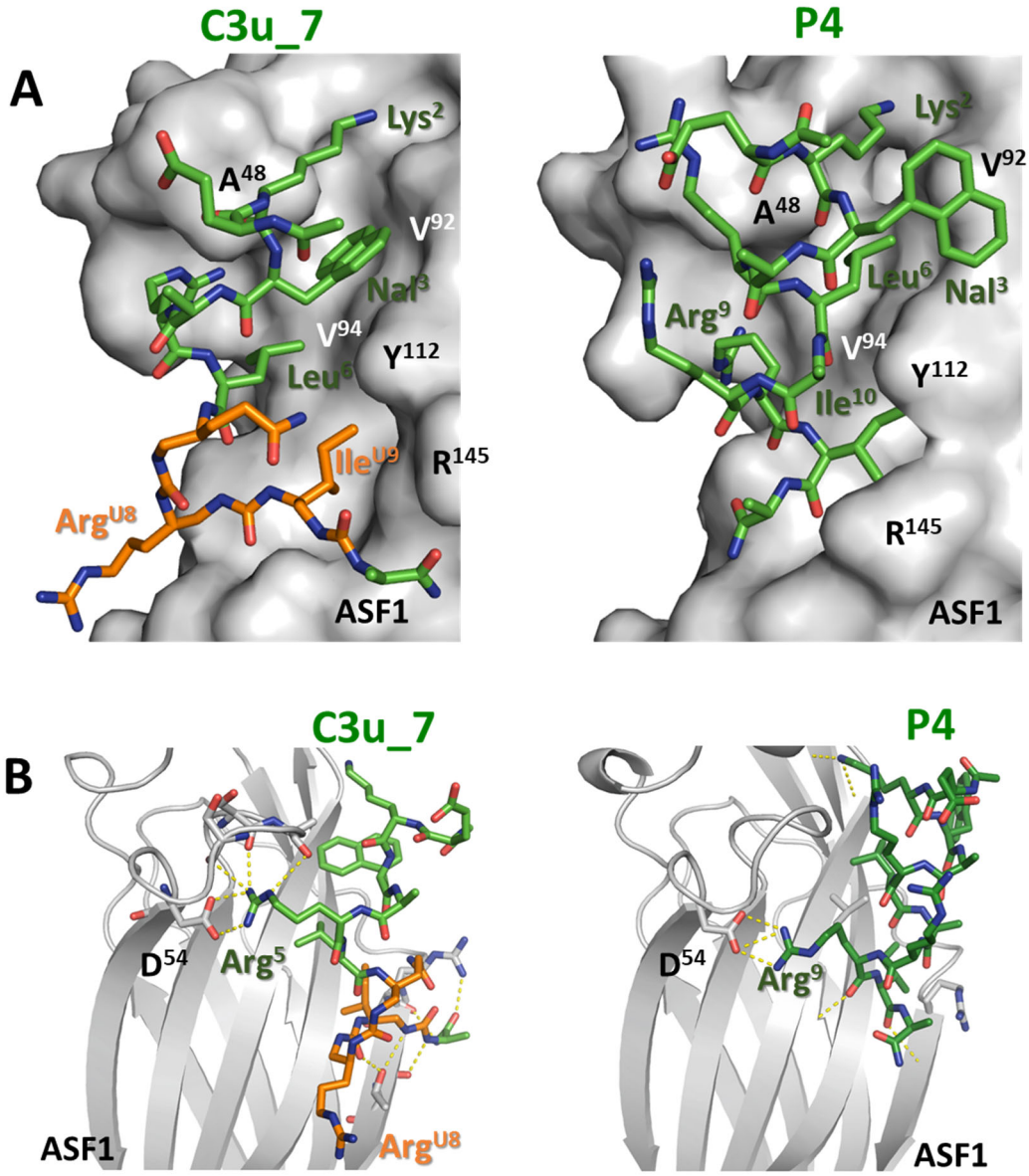

Supplementary Figure S9. Comparison between the binding mode of ASF1A$_N$-c3u_7 and ASF1A$_N$-P4 to ASF1. ASF1 is coloured in grey. The chimera inhibitors are coloured according to Figure 2 (representation in surface). ***Left panel***, ASF1A$_N$-**c3u_7** complex. ***Right panel***, ASF1A$_N$-**P4** complex. ***(A)*** View with the same orientation as in Fig. 5, ASF1 is shown as a surface. ***(B)*** View highlighting the salt bridge of the peptide/chimera with ASF1 D^{54}.

Chemical synthesis

Chemicals and general procedures

Commercially available reagents were used throughout without purification. THF, DCM were preliminary dried by passing through solvent drying system (SPS 800 Manual from MBraun). DMF and DCM for solid phase synthesis were purchased from Carlo ERBA. HPLC-grade quality acetonitrile (CH_3CN) and MilliQ water were used for RP-HPLC analyses and purification. N-protected amino acids were purchased from Iris Biotech, Fluorochem. Rink amide resin was purchased from Sigma-Merck laboratories.

Thin layer chromatography (TLC) was performed on silica gel 60 F254 (Merck) with detection by UV light and stain with 1% w/w ninhydrin in ethanol followed by heating. Flash column chromatography was carried out on silica gel (40-63 µm, Merck). ^{1}H NMR and ^{13}C NMR spectra were recorded on an Avance II NMR spectrometer (Bruker Biospin) with a vertical 7.05T narrowbore/ ultrashield magnet operating at 300 MHz for ^{1}H observation and 75 MHz for ^{13}C observation by means of a 5-mm direct BBO 1H/19F_XBB_H probe with Z gradient capabilities. Chemical shifts (δ) are reported in parts per million (ppm) relative to the ^{1}H or ^{13}C residual signal of the deuterated solvent used. ^{1}H NMR splitting patterns with observed first-order coupling are designated as singlet (s), broad signal (br), doublet (d), triplet (t), or quartet (q). Not defined ^{1}H NMR splitting patterns are designated as multiplet (m). Coupling constants (J) are reported in hertz (Hz). Electrospray high resolution mass spectrometry (ESI-HRMS) analyses were carried out on a Thermo Exactive with an ion trap mass analyzer from the Mass Spectrometry Facility at the European Institute of Chemistry and Biology (UMS 3033 - IECB), Pessac, France.

Solid phase peptide synthesis with microwave irradiation was carried out on the LibertyBlue system, from CEM (CEM µWaves S.A.S., Orsay, France). Solid phase oligourea synthesis with microwave irradiation was carried out on the DiscoverBio system, from CEM (CEM µWaves S.A.S., Orsay, France). Analytical RP-HPLC analyses were performed on a Dionex ultimate U3000SD using a Macherey-Nagel Nucleodur column (4.6 × 100 mm, 3 µm) at a flow rate of 1 mL/min. The mobile phase was composed of 0.1% (v/v) TFA in MilliQ water (Solvent A) and 0.1% TFA in CH_3CN (Solvent B). The detection was performed at 200 nm and the column temperature in the oven was 25 °C. Semi-preparative purifications of oligomers were performed on a Dionex ultimate U3000SD using a Macherey-Nagel Nucleodur VP250/10 100-16 C18ec column (10 × 250 mm, 16 µm) at a flow rate of 4 mL/min. Preparative purifications of oligomers were performed on a Gilson GX-281 using a Macherey-Nagel Nucleodur VP250/21 100-5 C18ec column (21 × 250 mm, 5 µm) at a flow rate of 20 mL/min. Column eluent was monitored by UV detection at 200, 214 and 254 nm. The purity of the analyzed compounds was determined to be ≥ 95% by using the data processing application of Chromoleon7 software. LC-MS analyses were carried out on an Agilent G6230B TOF spectrometer coupled with an Agilent HPLC system.

Structure of succinimidyl(2-azidoethyl)carbamate building blocks M1 – M7.

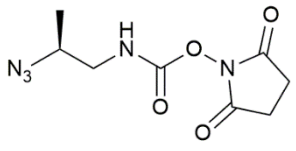

M1 (N_3-Ala^U-OSu)

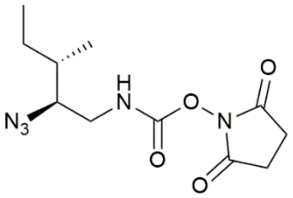

M2 (N_3-Ile^U-OSu)

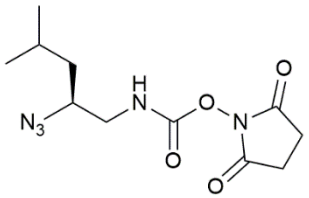

M3 (N_3-Leu^U-OSu)

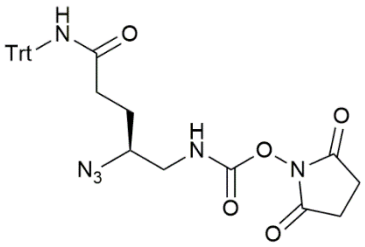

M4 (N_3-Gln^U-OSu)

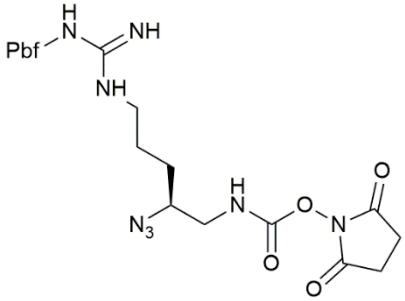

M5 (N_3-Arg^U-OSu)

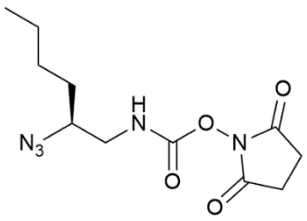

M6 (N_3-Nle^U-OSu)

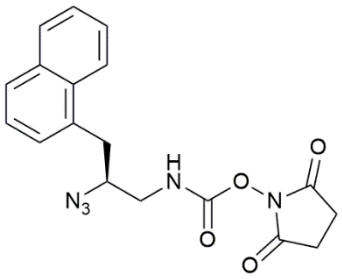

M7 (N_3-Nal^U-OSu)

Supplementary Figure S10. Monomer M1 – M7 needed to prepare 3-urea chimeras.

Building blocks M1 and M3 – M7

The synthesis of activated building blocks follows the previous described procedures for **M1** and **M3** – **M7** [1, 3-5]

Synthesis of M2 with Ile side chain.

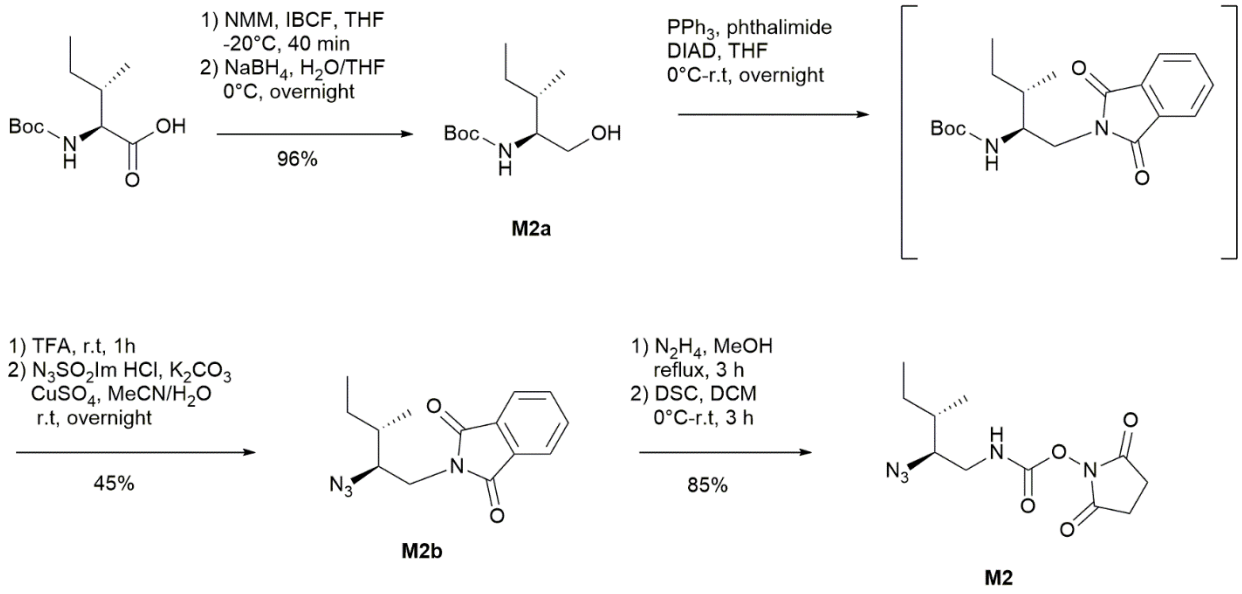

Supplementary Figure S11. Synthetic route of monomer M2.

(S)-tert-butyl (1-hydroxy-3-methylpentan-2-yl)carbamate **M2a**

The *N*-Boc-Ile-OH, $2H_2O$ (10.0 mmol, 2.7 g) was dissolved in anhydrous THF (50 mL) under N_2 atmosphere and cooled down to -20 °C. After addition of isobutyl chloroformate (12 mmol, 1.6 mL) and NMM (1.2 equiv., 12 mmol, 1.3 mL), the mixture was stirred at -20 °C for 40 min. The resulting white precipitate was filtered off and the filtrate was added at 0 °C to a solution of $NaBH_4$ (12 mmol, 0.454 g) in water (10 mL). The reaction mixture was let to react overnight and then quenched by addition of 1 M $KHSO_4$ aqueous solution. The THF was removed under reduced pressure and the aqueous solution was extracted 3 times with EtOAc. The organic layers were combined, washed two times with 1 M $KHSO_4$ solution, two times with saturated solution of $NaHCO_3$, one time with brine, dried over Na_2SO_4 and concentrated under reduced pressure. The crude residue was purified through silica gel flash chromatography (10 – 50 % EtOAc in Cyclohexane) to give N-Boc protected amino alcohol **M2a** as colorless oil (2.16 g, yield 96%). ^{1}H NMR (300 MHz, $CDCl_3$) δ 4.65 (s, 1H), 3.75 – 3.55 (m, 2H), 3.50 (d, J = 4.7 Hz, 1H), 1.45 (s, 9H), 1.42 (s, 2H), 1.20 – 1.09 (m, 1H), 0.93 (d, J = 2.4 Hz, 3H), 0.91 (d, J = 1.9 Hz, 3H).

(S)-2-(2-azido-3-methylpentyl) isoindoline-1,3-dione **M2b**

In a round bottom flask, triphenylphosphine (12 mmol, 3.13 g) and phthalimide (12 mmol, 1.76 g) were dissolved in anhydrous THF (60 mL) under N_2 atmosphere at 0 °C, followed by dropwise addition of DIAD (12 mmol, 2.4 mL). The mixture was stirred at 0°C for 10 min. *N*-Boc protected amino alcohol **M2a** (10 mmol, 2.16 g) in THF (20 mL) was added. The reaction mixture was allowed to warm-up to room temperature and stirred overnight. After concentration under reduced pressure, the crude residue was used directly for next step without purification. The crude phthalimide

derivative was dissolved in pure TFA (10 mL) and let to react for 1 h. TFA was removed under reduced pressure and to the residue HCl solution in diethyl ether (2M) was added and the white solid was filtered and collected. After drying on vacuum line, the crude product was engaged in the next step. To a solution of the crude product in CH_3CN/H_2O (1:1 v/v, 200 mL) were added K_2CO_3 (27 mmol, 3.73g), imidazole-1-sulfonyl azide hydrochloride ($N_3SO_2Im.HCl$) (12 mmol, 2.52 g) and $CuSO_4.5H_2O$ (0.1 mmol, 25 mg). The mixture was stirred at room temperature overnight. After concentration under reduced pressure, EtOAc was added. The organic phase was washed two times with 1 M $KHSO_4$ aqueous solution, once with brine, dried over Na_2SO_4 and concentrated under reduced pressure. After silica gel flash chromatography, the desired pure product was obtained as colorless oil (1.3 g, yield 47% over 3 steps). ^{1}H NMR (300 MHz, $CDCl_3$) δ 7.98 – 7.33 (m, 4H), 3.64 (s, 1H), 2.27 (dd, *J* = 58.3, 15.9 Hz, 1H), 1.57 (s, 2H), 1.40 (d, *J* = 15.0 Hz, 2H), 1.18 – 1.00 (m, 3H), 0.98 – 0.72 (m, 3H).

(S)-2,5-dioxopyrrolidin-1-yl (2-azido-3-methylpentyl) carbamate **M2**

To a solution of *(S)* - 2-(2-azido-3-methylpentyl) isoindoline-1,3-dione **M2b** (4.8 mmol, 1.3 g,) in MeOH (50 mL), hydrazine hydrate (14.4 mmol, 710 µL) was added. The reaction mixture was heat to reflux and maintained for 3 h under stirring. The white precipitate was filtered off, washed with MeOH and the filtrate was concentrated under reduced pressure. The crude residue was dissolved in EtOAc and filtered again. The filtrate was washed three times with 0.5 M HCl solution. The combined aqueous phases were again washed with EtOAc and then neutralized by addition of K_2CO_3 until pH > 8. The aqueous phase was finally extracted with DCM and the combined organic layers were dried over Na_2SO_4, concentrated under reduced pressure but not until dryness. The resulting amine was directly used for next step and added to a stirred suspension of disuccinimidyl carbonate (5.76 mmol, 1.48 g) in anhydrous DCM at 0 °C. The reaction mixture was stirred 3 h at room temperature and was concentrated under reduced pressure. The crude residue was dissolved in EtOAc and the organic phase was washed two times with 1 M $KHSO_4$ aqueous solution, one with brine and dried over Na_2SO_4, followed by concentration under reduced pressure. The product was precipitated in a cold mixture of pentane/Et_2O (3:7, v/v) giving the monomer **M2** as white solid (1.16g, yield 85% for two steps). ^{1}H NMR (300 MHz, $CDCl_3$) δ 5.51 (s, 1H), 3.60 – 3.41 (m, 2H), 3.17 – 3.02 (m, 1H), 2.81 (s, 4H), 1.74 – 1.61 (m, 1H), 1.54 – 1.41 (m, 1H), 1.34 – 1.14 (m, 1H), 1.01 – 0.87 (m, 6H). ^{13}C NMR (75 MHz, $CDCl_3$) δ 169.95, 151.64, 77.50, 77.08, 76.66, 66.62, 42.97, 37.18, 25.49, 25.46, 15.07, 11.39. HRMS (ESI-TOFMS) *m/z* calcd. for $C_{11}H_{21}N_6O_4$ $[M+NH_4]^+$ 301.1619, found 301.1618

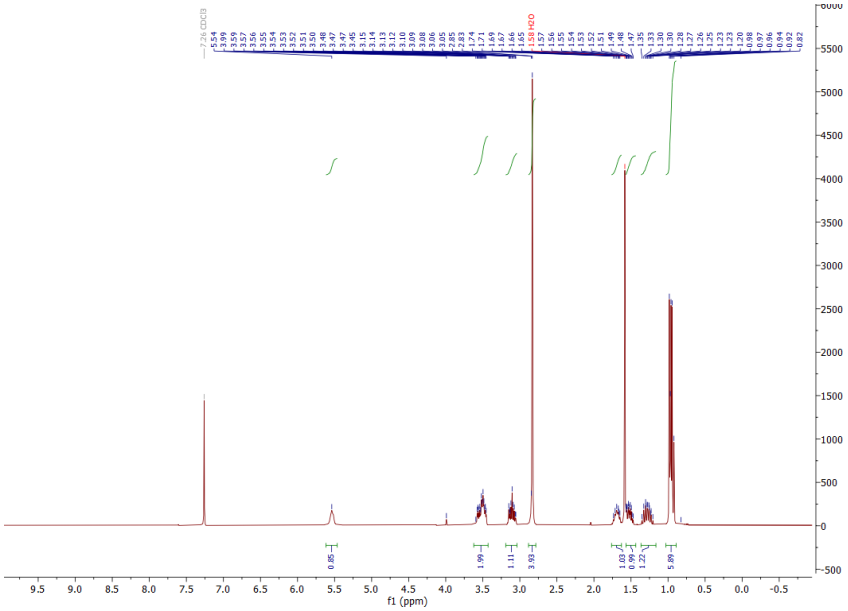

Supplementary Figure S12. ^{1}H NMR spectrum of monomer M2.

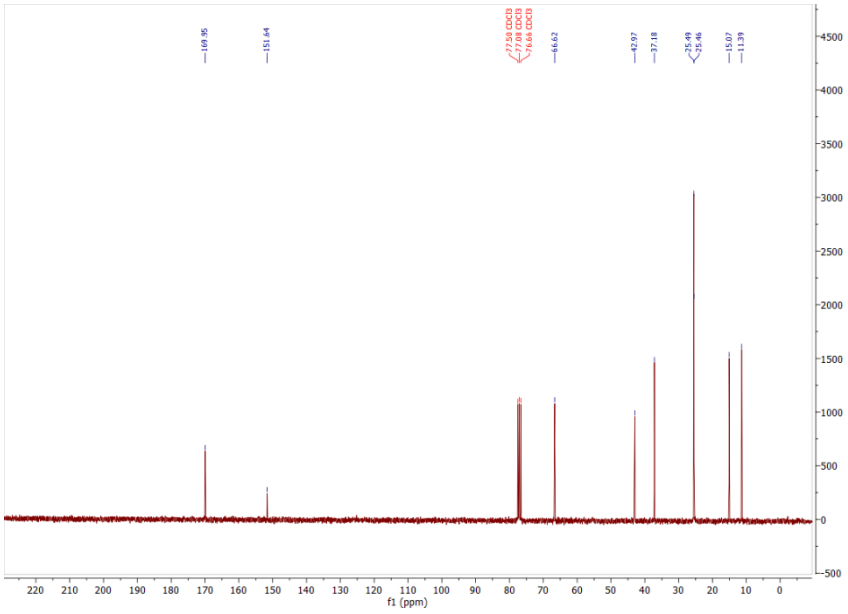

Supplementary Figure S13. ^{13}C NMR spectrum of monomer M2.

Oligomer synthesis

The peptide-urea-hybrid oligomers were synthesized on a 50 to 100 µmol scale. Polystyrene Rink amide MBHA resin (100 – 200 mesh) was placed in the reaction vessel, and preswollen with DMF for 1 – 2 hours. All steps were performed under inert atmosphere (N_2) and microwave irradiation on either the discover Liberty Blue or Bio system (CEM). The vessel was then placed inside the microwave oven. The temperature was maintained by modulation of power and controlled with a fiber optic sensor.

General procedures for Fmoc deprotection and peptide coupling

Fmoc removal was carried out with 20% of piperidine in DMF under microwave irradiation (155 W, 75 °C, 15 s + 30 W, 90 °C, 110 s). Fmoc-Xaa-OH (5 equiv., relative to the resin loading), DIC (5 equiv., relative to the resin loading) Oxyma (5 equiv., relative to the resin loading) were dissolved in DMF. The mixture was added into the reaction vessel (Liberty Blue). The Fmoc-AA-OH (except Fmoc-Arg(Pbf)-OH) was coupled twice under microwave irradiation with standard coupling method (170 W, 75 °C, 15 s + 30 W, 90 °C, 110 s). The coupling of Fmoc-Arg(Pbf)-OH was performed by conventional peptide coupling (0 W, 25 °C, 25 min + 25 W, 75 °C, 120 s). The coupling procedure was repeated once as well. The resin was then filtered off and washed with DMF twice.

General procedures for urea coupling and azide reduction

The azido protected monomer (N_3-Xaa^U-OSu) (1.5 equiv., relative to the resin loading) and DIEA (3.0 equiv., relative to the resin loading) were dissolved in DMF. This mixture was added into the reaction vessel (CEM) and bubbled with N_2 gas for several seconds. The reaction vessel was then irradiated under microwave (Liberty Bio system) (70 °C, 30 W, 20 min). A double coupling was performed systematically. The resin was then filtered off, washed with DMF (3 mL x 3) and with a mixture of 1,4-dioxane/H_2O (7:3, v/v, 4 mL x 3). The azido group was reduced via Staudinger reduction reaction under microwave. The resin was swollen in 1,4-dioxane/H_2O mixture followed by addition of 1 M PMe_3 solution in THF (10 equiv., relative to the resin loading). Then the reaction vessel was irradiated under microwave (50 °C, 30 W, 15 min). The reduction process was performed systematically twice. The resin was then filtered off and washed with DMF (3 mL x 4). These coupling and reduction steps were monitored with a chloranil test.

General procedure for acetyl capping and cleavage

Final acetylation was performed with a mixture of acetic anhydride (0.5 mL) and DIEA (10 equiv. relative to the resin loading) in 2 mL DMF by shaking at room temperature for 1 hour. The resin was then filtered off and washed with DMF (3 mL x 2) and CH_2Cl_2 (3 mL x 2). To cleave the oligomer from the resin simultaneously with protecting group removal, the resin was swollen in a mixture of TFA/TIS/H_2O (95:2.5:2.5, v/v/v) and let to react for 3 h under shaking, then filtered off, washed with TFA (2 x 2 mL) and CH_2Cl_2 (2 x 2 mL). The filtrate was evaporated under reduced pressure and precipitated in cold Et_2O. The crude oligomer was lyophilized, analyzed on RP-HPLC before to be purified by preparative or semi-preparative RP-HPLC using an appropriate gradient to a final purity ≥95%.

HPLC and LCMS of the foldamers c3u (for chimera containing 3 ureas)

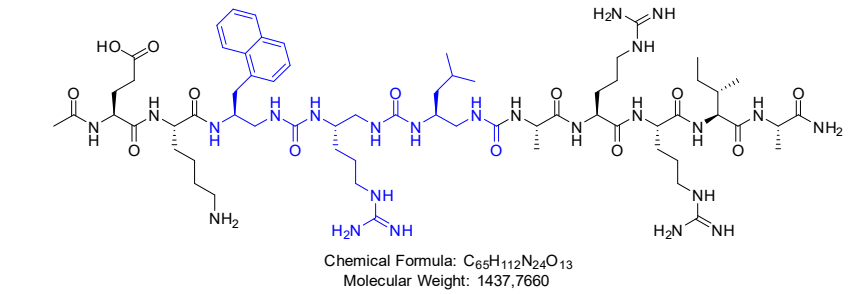

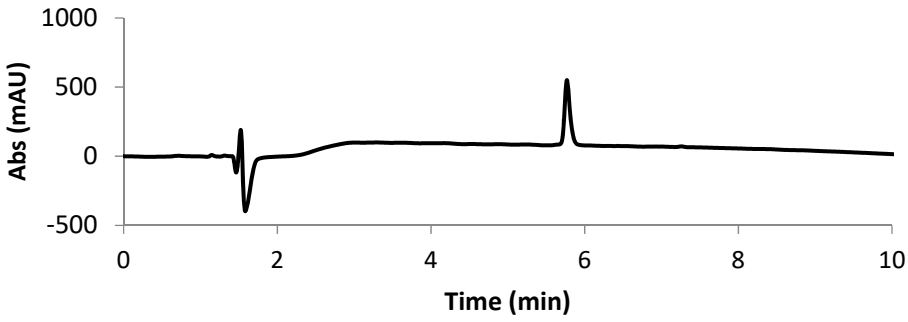

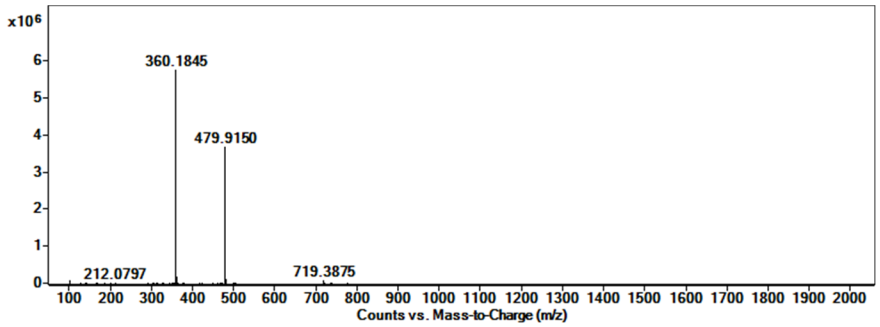

Supplementary Figure S14. Synthesis of c3u_3 chimera. ***Top***, chemical sequence Ac-EK-{L-1Nal}^{U}R^{U}L^{U}ARRIA-NH_2. Synthesis from 50 µmol scale, after purification giving 20.2 mg, 28% yield. ***Middle***, HPLC: 10-60% line B, 50 °C, 10 min, λ = 200 nm, t_R = 5.77 min. ***Bottom***, MS (ESI$^+$): (*m/z*) = 360.1845 $[M+4H]^{4+}$; 479.9150 $[M+3H]^{3+}$.

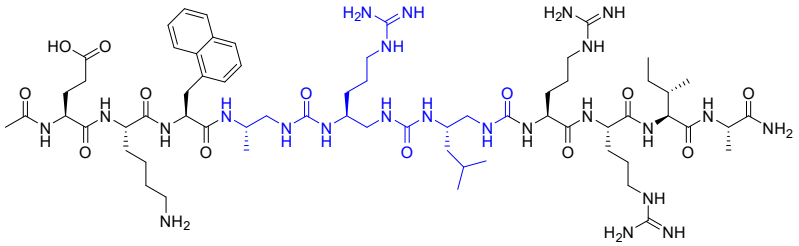

Chemical Formula: $C_{65}H_{112}N_{24}O_{13}$
Molecular Weight: 1437,7660

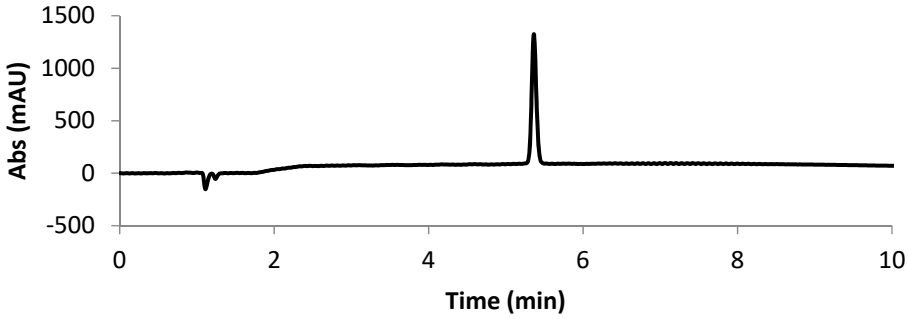

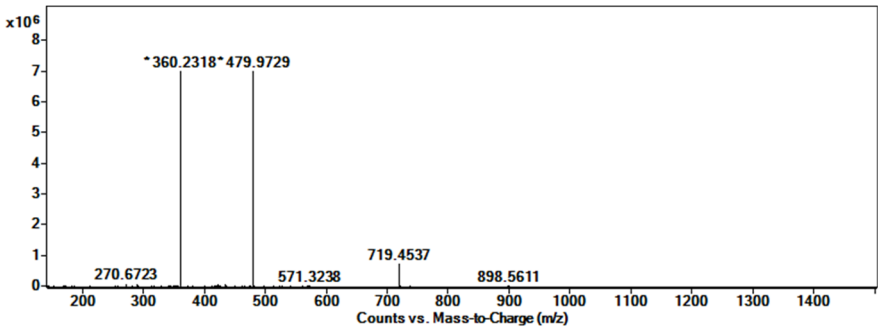

Supplementary Figure S15. Synthesis of c3u_4 chimera. ***Top***, chemical sequence Ac-EK{1Nal}A^{U}R^{U}L^{U}RRIA-NH_2. Synthesis from 70 µmol scale, after purification giving 57 mg, 57% yield. ***Middle***, HPLC: 10-60% line B, 25 °C, 10 min, λ = 200 nm, t_R = 5.36 min. ***Bottom***, MS (ESI$^+$): (*m/z*) = 360.2318 $[M+4H]^{4+}$; 479.9729 $[M+3H]^{3+}$; 719.4537 $[M+2H]^{2+}$.

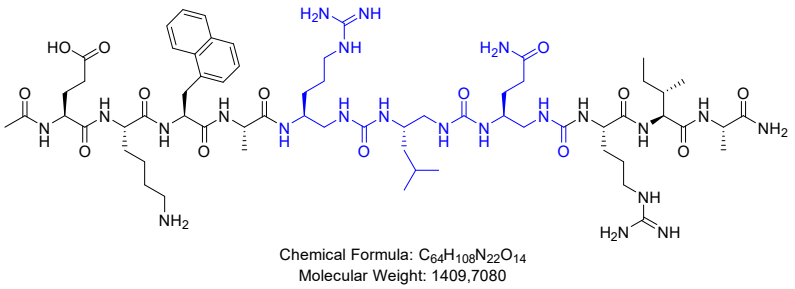

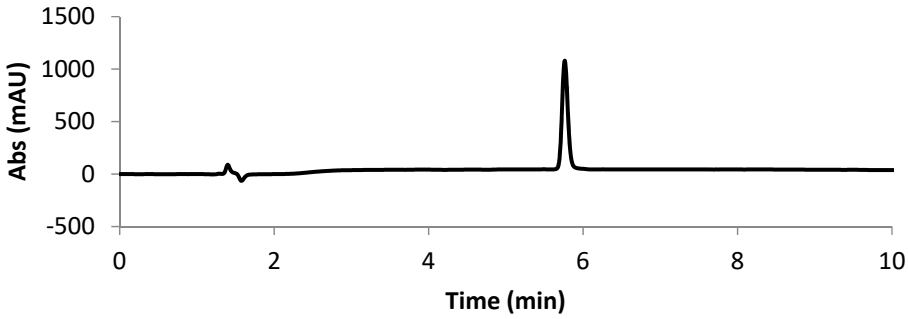

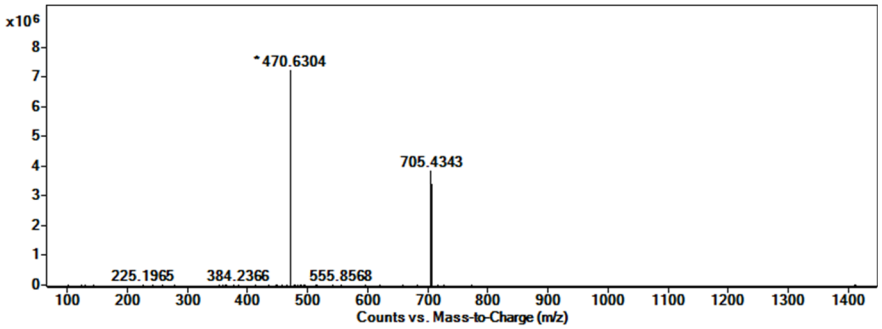

Supplementary Figure S16. Synthesis of c3u_5 chimera. ***Top***, chemical sequence Ac-EK{1Nal}AR^{U}L^{U}Q^{U}RIA-NH_2. Synthesis from 50 µmol scale, after purification giving 10.3 mg, 19.6% yield. ***Middle***, HPLC: 20-50% line B, 25 °C, 10 min, λ = 200 nm, t_R = 5.76 min. ***Bottom***, MS (ESI$^+$): (*m/z*) = 470.6304 $[M+3H]^{3+;}$ 705.4343 $[M+2H]^{2+}$.

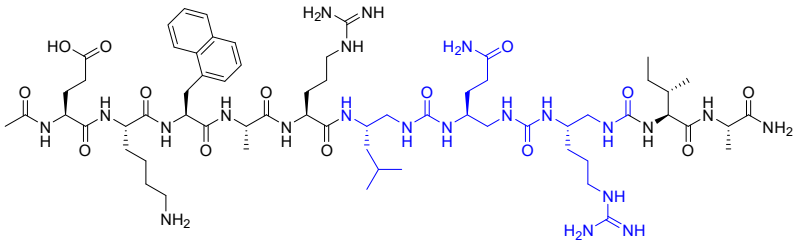

Chemical Formula: $C_{64}H_{108}N_{22}O_{14}$
Molecular Weight: 1409,7080

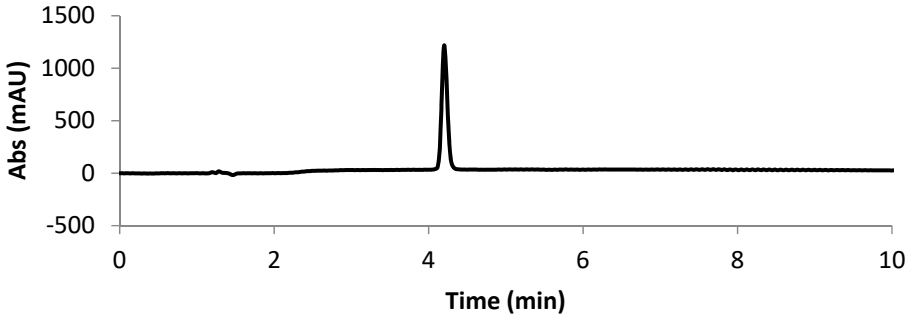

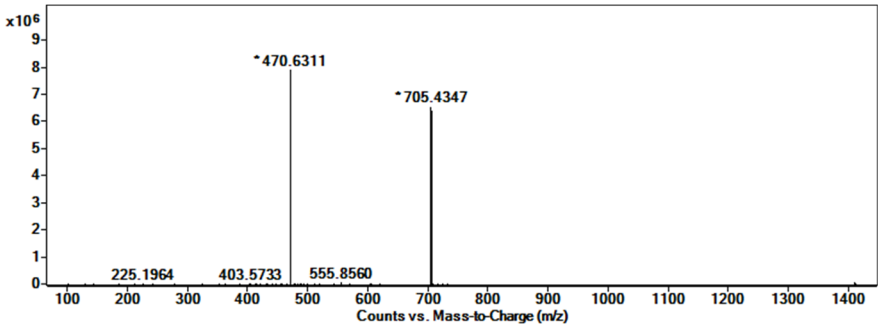

Supplementary Figure S17. Synthesis of c3u_6 chimera. ***Top***, chemical sequence Ac-EK{1Nal}ARL^{U}Q^{U}R^{U}IA-NH_2. Synthesis from 50 µmol scale, after purification giving 16 mg, 22.7% yield. ***Middle***, HPLC: 20-50% line B, 25 °C, 10 min, λ = 200 nm, t_R = 4.20 min. ***Bottom***, MS (ESI$^+$): (*m/z*) = 470.6311 $[M+3H]^{3+;}$ 705.4347 $[M+2H]^{2+}$.

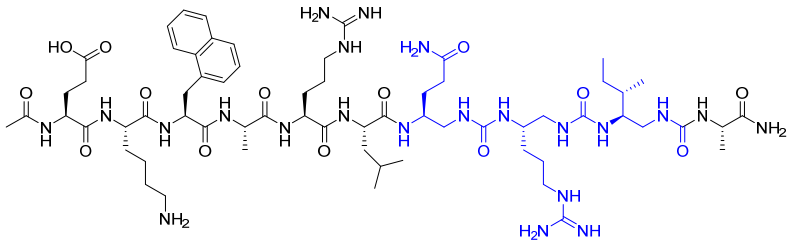

Chemical Formula: $C_{64}H_{108}N_{22}O_{14}$
Molecular Weight: 1409,7080

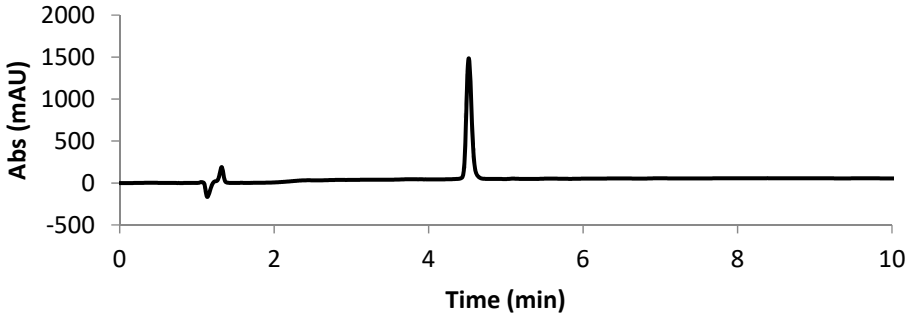

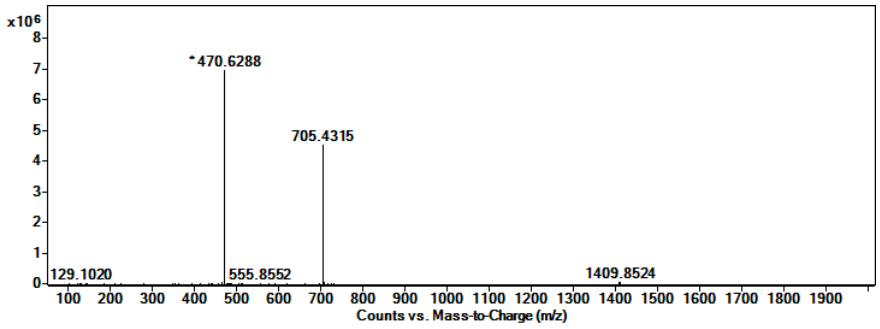

Supplementary Figure S18. Synthesis of c3u_7 chimera. ***Top***, chemical sequence Ac-EK{1Nal}ARLQ^{U}R^{U}I^{U}A-NH_2. Synthesis from 50 µmol scale, after purification giving 14.4 mg, 20.3% yield. ***Middle***, HPLC: 20-50% line B, 25 °C, 10 min, λ = 200 nm, t_R = 4.52 min. ***Bottom***, MS (ESI$^+$): (*m/z*) = 470.6288 $[M+3H]^{3+}$; 705.4315 $[M+2H]^{2+}$.

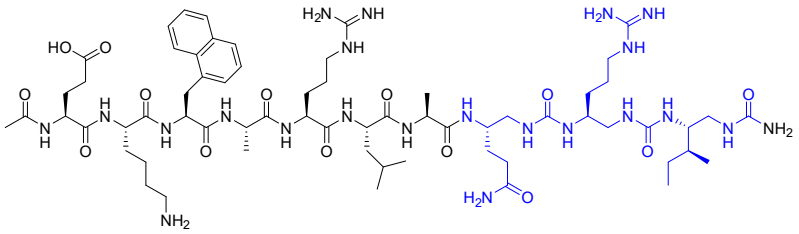

Chemical Formula: $C_{64}H_{108}N_{22}O_{14}$
Molecular Weight: 1409,7080

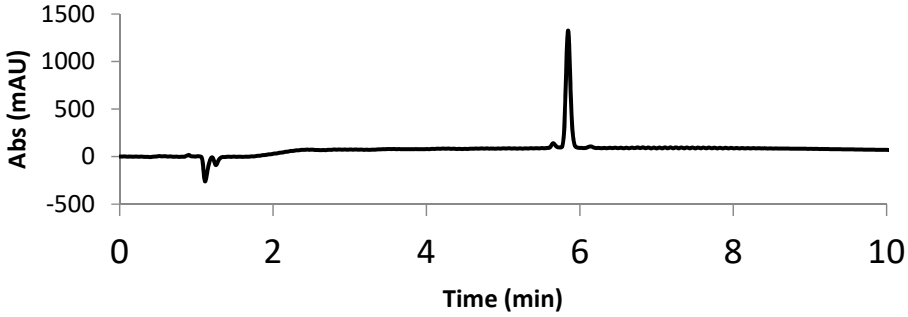

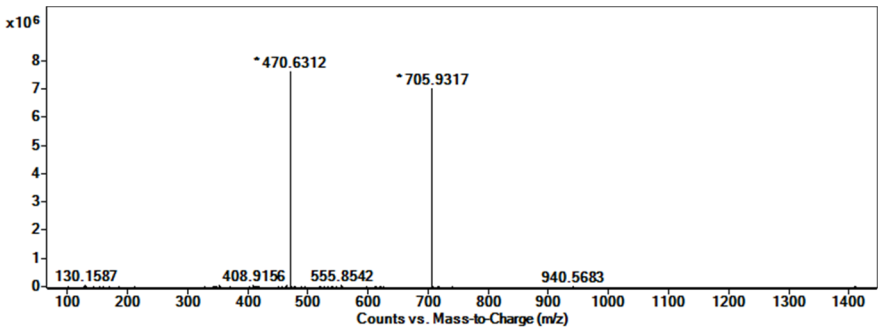

Supplementary Figure S20. Synthesis of c3u_8 chimera. ***Top***, chemical sequence Ac-EK{1Nal}ARLAQ^{U}R^{U}I^{U}-NH_2. Synthesis from 75 µmol scale, after purification giving 43.5 mg, 43.3% yield. ***Middle***, HPLC: 10-60% line B, 25 °C, 10 min, λ = 200 nm, t_R = 5.85 min. ***Bottom***, MS (ESI$^+$): (*m/z*) = 470.6312 $[M+3H]^{3+}$; 705.9317 $[M+2H]^{2+}$.

Expression and purification of ASF1

Recombinant human ASF1 [hASF1A(1-156)] was purified as already described from expression in Escherichia coli of a $(His)_6$–glutathione S-transferase (GST)–TEV site–Asf1 fusion protein using the pETM30 plasmid. Briefly, soluble $(His)_6$-tagged GST fusion protein was purified on reduced glutathione agarose beads (Sigma-Aldrich). After cleavage with recombinant (His)6-Tobacco Etch Virus Protease (TEV) protease at room temperature overnight, the (His)6-GST tag and the protease were trapped in a nickel-charged nitrilotriacetic acid (NiNTA) chelate immobilized onto agarose column (Macherey Nagel). The flow-through fraction containing ASF1 protein was further purified by anion exchange chromatography using a Resource Q 6-ml column (GE Healthcare). ASF1 was then concentrated using an Amicon device (Millipore), and the buffer was replaced with a 50 mM Tris-HCl pH 7.5 buffer. Unlabeled ASF1 used for ITC experiments was purified from pellets of bacteria grown in LB medium and uniformly labeled ASF1 from bacteria grown in M9 minimal media supplemented with $(^{15}NH_4)Cl$ (0.5 g/liter; Eurisotop) as the sole nitrogen source [6].

Isothermal titration calorimetry (ITC)

All ITC experiments were performed on a VP-ITC titration calorimeter (Microcal/Malvern) at 20°C, in a 50 mM Tris-HCl (pH 7.5) buffer. Protein and peptides concentrations were set to values ranging from 10 to 580 µM. Each foldamer was titrated with an optimal protein : peptide ratio, in order to get the optimal transition for minimizing the fitting errors. Protein and peptide samples were prepared in the same buffer and degassed for 5 min by sonication or vacuum. After equilibrating the cell at 293.15°K, the rotating syringe (310 rpm) injected at intervals of 180 s, 10 µL of aliquots (30 injections overall) of peptide solution into the ASF1 solution previously introduced in the sample cell, until saturation was observed. Raw ITC data were processed with the Origin 7.0 Software (OriginLab, Malvern) using the One-Set of Sites fitting model. All ITC experiments were performed at least in duplicate. One representative curve for each peptide/chimera is shown in Figure S2.

Conformation of free chimera by NMR experiments and molecular modeling

NMR experiments were carried out on Bruker DRX-700 spectrometer. The chimera were concentrated at 1.5mM in the buffer (10mM Phosphate pH 6, 0.1 mM EDTA, 0.1; mM DSS, 0.1;mM NaN_3, 5% D_2O). Complete assignment was obtained at three temperatures (283°K, 293°K and 303°K) with homonuclear TOCSY (80 ms and 10 ms mixing times) and NOESY (150 and 300ms mixing times) experiments and heteronuclear experiments with natural abundance of ^{13}C and ^{15}N isotopes: sofast-HMQC and edited HSQC in the aliphatic and aromatic frequency ranges. Proton chemical shifts (in ppm) were referenced relative to internal DSS and ^{15}N and ^{13}C references were set indirectly relative to DSS using frequency ratios [7]. NMR data were processed using Topspin (Bruker) and analyzed using Sparky (T.D. Goddard and D.G. Kneller, UCSF). Values for random coiled chemical shifts used in the calculation of secondary Cα were taken from a study by [2, 8]. Molecular models of the chimera were built according to the regular structure of urea helices and expected H-bond network for transitions between the oligourea and peptide segments [9]. The complete set of hydrogen bonds is reported in table S4.

Chemical shift mapping of ASF1 upon chimera binding

The binding mode of chimera was assessed using NMR spectroscopy following the amide chemical shifts of ASF1 residues. NMR experiments were performed at 293°K on Bruker Avance II 600 MHz spectrometer equipped with a

proton-optimized triple resonance NMR 'inverse' cryoprobe (TCI), (Bruker). Purified uniformly labeled ^{15}N hASF1A(1-156) was concentrated to 50 µM and exchanged with the buffer [50 mM Tris-HCl (pH 7.5), 0.1 mM EDTA, 0.1 mM dextran sulfate sodium (DSS), 0.1 mM NaN_3, protease inhibitor cocktail (at the concentration recommended by the provider, Roche), and 10% D_2O]. Proton chemical shifts (in parts per million) were referenced relative to internal DSS, and ^{15}N reference was set indirectly relative to DSS using frequency ratios. NMR data were processed using Topspin (Bruker) and analyzed using Sparky (T. D. Goddard and D. G. Kneller, University of California San Francisco). Amide assignment was taken from our previous assignment.[6] The titration experiments were performed by adding increasing amounts of concentrated peptide or chimera to the ASF1 sample. At each new ASF1 : peptide ratio, a two dimensional ^{1}H-^{15}N SOFAST HMQC (heteronuclear multiple-quantum coherence) spectrum was recorded. Changes in chemical shift were measured for all resonances for all recorded spectra. Assignments were obtained by following progressive variations of chemical shifts upon titration. Chemical shift variation was calculated with the following formula: $\Delta\delta = \sqrt{\left(\delta_{HN}^{b} - \delta_{HN}^{f}\right)^2 + \left(0.17\left(\delta_{N}^{b} - \delta_{N}^{f}\right)\right)^2}$, where δ represents measured chemical shift value. b or f refer to the bound or free forms, respectively, HN or N to the amide proton or nitrogen, respectively. The factor 0.17 corresponds to the scaling factors used to normalize the magnitude of the proton and nitrogen chemical shift changes (in parts per million) [7, 10]. At saturation of the peptide or chimera, the maximal chemical shift variation was plotted as a function of the residue number for 138 residues of the 156 residues of hASF1A(1-156) (Fig. S3). This corresponds to 96% of the expected values, considering the 12 prolines. The exchange rate between bound and free forms was rapid upon addition of all chimeras c3u_i, and of the chimera c4u. Conversely, this exchange rate was slow upon the addition of P4 to $ASF1_N$.

X-ray diffraction

$ASF1A_N$ was concentrated as indicated in Table S1 and Table S5 in a buffer solution of 50 mM Tris-HCl pH 7.5. $ASF1A_N$-chimera were mixed at a given ratio to form the corresponding complex, as stated in Table S1 and Table S5. The final volume of mixture solution included 10% of inhibitor protease cocktail at the concentration recommended by the manufacturer (cOmplete, Roche). Crystals of complex were grown by sitting drop vapour diffusion at 17°C against their own reservoir solution. If noticed, crystals were soaked in a cryoprotectant made of 12% glycerol in solution in the corresponding reservoir solution, before being flash frozen in liquid nitrogen. Diffraction data were collected on the PROXIMA-1 and PROXIMA-2 beamlines at the synchrotron SOLEIL (Saint Aubin, France) at a temperature of 100°K with X-ray wavelength of 0.97857 Å. Diffraction images recorded with PILATUS 6M detector were processed using the XDS package.[11] Structures of ASF1-foldamer complexes were solved by molecular replacement using PHENIX with the human ASF1A structure (chain A of Protein Data Bank, PDB entry: 2IO5) as model probe. [12] Structure model and related mmCIF files for unnatural monomers were generated on the Grade Web Server (http://grade.globalphasing.org). Model building was performed manually with Coot version 0.8.9.1 [13, 14]} and structure refinement was achieved with BUSTER version 2.10.4. [15, 16] The models were validated with MolProbity. The statistic tables for the $ASF1_N$–P4 complex (Table S1), and for the $ASF1_N$–**c3u_3**, $ASF1_N$–**c3u_5**, and $ASF1_N$–**c3u_7** complexes (Table S5) recapitulate the main parameters of data collection and model refinement. Structure representations presented in all figures were drawn with PyMOL software (Schrödinger).

References

1. J. Mbianda, M. Bakail, C. Andre, G. Moal, M. E. Perrin, G. Pinna, R. Guerois, F. Becher, P. Legrand, S. Traore, C. Douat, G. Guichard and F. Ochsenbein, *Sci Adv*, 2021, **7**.
2. K. Tamiola, B. Acar and F. A. Mulder, *J Am Chem Soc*, 2010, **132**, 18000-18003.
3. C. Douat-Casassus, K. Pulka, P. Claudon and G. Guichard, *Org Lett*, 2012, **14**, 3130-3133.
4. G. W. Collie, C. M. Lombardo, S. H. Yoo, K. Pulka-Ziach, V. Gabelica, C. D. Mackereth, F. Rosu and G. Guichard, *Chem Commun (Camb)*, 2021, **57**, 9514-9517.
5. L. Cussol, L. Mauran-Ambrosino, J. Buratto, A. Y. Belorusova, M. Neuville, J. Osz, S. Fribourg, J. Fremaux, C. Dolain, S. R. Goudreau, N. Rochel and G. Guichard, *Angew Chem Int Ed Engl*, 2021, **60**, 2296-2303.
6. F. Mousson, J. Couprie, J. Y. Thuret, J. M. Neumann, C. Mann and F. Ochsenbein, *J Biomol NMR*, 2004, **29**, 413-414.
7. D. S. Wishart, C. G. Bigam, J. Yao, F. Abildgaard, H. J. Dyson, E. Oldfield, J. L. Markley and B. D. Sykes, *J Biomol NMR*, 1995, **6**, 135-140.
8. D. S. Wishart, C. G. Bigam, A. Holm, R. S. Hodges and B. D. Sykes, *J Biomol NMR*, 1995, **5**, 332.
9. J. Fremaux, L. Mauran, K. Pulka-Ziach, B. Kauffmann, B. Odaert and G. Guichard, *Angew Chem Int Ed Engl*, 2015, **54**, 9816-9820.
10. B. T. Farmer, 2nd, K. L. Constantine, V. Goldfarb, M. S. Friedrichs, M. Wittekind, J. Yanchunas, Jr., J. G. Robertson and L. Mueller, *Nat Struct Biol*, 1996, **3**, 995-997.
11. W. Kabsch, *Acta Crystallogr D Biol Crystallogr*, 2010, **66**, 133-144.
12. D. Liebschner, P. V. Afonine, M. L. Baker, G. Bunkoczi, V. B. Chen, T. I. Croll, B. Hintze, L. W. Hung, S. Jain, A. J. McCoy, N. W. Moriarty, R. D. Oeffner, B. K. Poon, M. G. Prisant, R. J. Read, J. S. Richardson, D. C. Richardson, M. D. Sammito, O. V. Sobolev, D. H. Stockwell, T. C. Terwilliger, A. G. Urzhumtsev, L. L. Videau, C. J. Williams and P. D. Adams, *Acta Crystallogr D Struct Biol*, 2019, **75**, 861-877.
13. P. Emsley and K. Cowtan, *Acta Crystallogr D Biol Crystallogr*, 2004, **60**, 2126-2132.
14. A. Casanal, B. Lohkamp and P. Emsley, *Protein Sci*, 2020, **29**, 1069-1078.
15. G. Bricogne, E. Blanc, M. Brandl, C. Flensburg, P. Keller, W. Paciorek, P. Roversi, A. Sharff, O. S. Smart, C. Vonrhein and T. O. Womack, *Cambridge, United Kingdom: Global Phasing Ltd.*, 2017.
16. O. S. Smart, T. O. Womack, C. Flensburg, P. Keller, W. Paciorek, A. Sharff, C. Vonrhein and G. Bricogne, *Acta Crystallogr D Biol Crystallogr*, 2012, **68**, 368-380.